1965

Operating characteristics of a cloud chamber suited for condensation measurements

Donald L. Packwood

OPERATING CHARACTERISTICS OF A CLOUD CHAMBER SUITED FOR CONDENSATION MEASUREMENTS

BY

DONALD L. PACKWOOD

AN

ABSTRACT

submitted to the faculity of the

UNIVERSITY OF MISSOURI AT ROLLA

in partial fulfillment of the requirements for the

Degree of

MASTER OF SCIENCE IN PHYSICS

Rolla, Missouri

1965

OPERATING CHARACTERISTICS OF A CLOUD CHAMBER SUITED FOR CONDENSATION MEASUREMENTS

A study has been made of the various errors encountered in the measurement of the homogeneous nucleation rate of water. A complete analysis of the propagation of errors has been made of the procedure for obtaining supersaturations. The error in measuring nucleation rates from the resulting error in measuring supersaturations has been estimated.

From this knowledge experiments have been performed in an attempt to minimize the errors in measuring homogeneous nucleation rates.

It was found to be impossible to measure temperatures in a supersaturated vapor. In order to obtain the initial temperatures, the steady state thermal gradient in the chamber was mapped. From this knowledge, it is possible to ascertain the temperature at any point near the center. A test was also made of the validity of using the adiabatic law

$$T_2 = T_1 \left(\frac{P_1}{P_2}\right)^{\frac{1-\gamma}{\gamma}}$$

to find the final temperature in the chamber.

Associated with this, an attempt was made to measure γ for the system more accurately.

Finally a measurement was performed to determine the time required for the chamber to return to equilibrium after an expansion.

OPERATING CHARACTERISTICS OF A CLOUD CHAMBER SUITED FOR CONDENSATION MEASUREMENTS

BY

DONALD L. PACKWOOD

A

THESIS

submitted to the faculity of the

UNIVERSITY OF MISSOURI AT ROLLA

in partial fulfillment of the requirements for the

Degree of

MASTER OF SCIENCE IN PHYSICS

Rolla, Missouri

1965

Approved by

James L. Kassner Jr. (advisor) Otto H. Hill

Ralph E. Lee K. G. Mayhan

ACKNOWLEDGEMENTS

The author wishes to thank his advisor, Dr. James L. Kassner, Jr. for the guidance and assistance in conducting this research. Being associated with Dr. Kassner has been a very rewarding experience.

Gratitude is extended to the author's co-workers; Lt. Edward F. Allard, Louis B. Allen, Ronald Dawbarn, Michael A. Grayson, and Raymond J. Schmitt for their assistance and many helpful suggestions during the course of this research. The author also wishes to thank Carl M. Lund, Cheryl A. Mueller, and Brunn W. Roysden for their contributions to this work. Appreciation is also expressed to Robert P. Madding and Eric O. Puronen, who successfully spotwelded the 0.0005 inch wire thermocouples used in this research.

Finally, the author wishes to thank his wife, Lona L. Packwood, for relieving him of the burden of typing this thesis.

This research was supported by the Atmospheric Sciences Section of the National Science Foundation, NSF Grants G-17994 and GP-2893.

TABLE OF CONTENTS

LIST OF FIGURES

FIGURE PAGE

LIST OF TABLES

CHAPTER I

INTRODUCTION

1. HISTORICAL BACKGROUND. Although the cloud chamber has been an important research tool for over sixty years and has contributed greatly to our knowledge of elementary particles, the fundamental processes encountered in its operation (the formation and rapid growth of drops in a supersaturated vapor and the heat flow from the walls) are not yet well understood. The cloud chamber facility at the University of Missouri at Rolla, is presently being used to study the homogeneous nucleation of water droplets. As a result it is necessary to have a reasonably thorough knowledge of some of the basic thermodynamic processes.

2. DEVICES WHICH ARE USED TO STUDY NUCLEATION PHENOMENA. There are many devices which could be used to study the nucleation of vapors. Steam nozzles, shock tubes, and wind tunnels are all used to study nucleation phenomena, but all of these devices present one limitation or another. Over a period of years a new cloud chamber technique has been developed in this laboratory by Mettenburg[1], Rinker[2], and Hughes[3]. Allard[4] adapted and extended this technique to the study of condensation phenomena. He found it to be an excellent device for studying homogeneous nucleation rates.

3. REVIEW OF CAPABILITIES AND LIMITATIONS OF CLOUD CHAMBER. At this point, it is important to review the capa-

bilities and limitations of the cloud chamber for work of this type. The cloud chamber is basically a device for creating a condition of supersaturation of a vapor in a gas-vapor mixture. It is necessary to have a precise knowledge of the degree of supersaturation attained. It would be desirable to determine the supersaturation directly from temperature measurement. However, this is not possible because condensation takes place on the sensing element with the consequent liberation of latent heat which causes an erroneous temperature reading. Since the vapor is usually a minor constituent of the gas-vapor mixture, the mixture behaves very nearly like a perfect gas. Thus, the degree of supersaturation is usually calculated from the pressure ratio or the expansion ratio by utilizing one of the forms of the adiabatic law. It is this procedure which draws criticism.[5,6] In order to see why, let us examine the processes taking place.

When the cloud chamber expands, the gas-vapor mixture is cooled to a temperature much lower than the temperature of the walls of the chamber, which remain at room temperature. Heat immediately flows in from the walls. As the gas next to the walls warms, it also expands. The resulting expansion of this boundary layer compresses the entire volume of gas and thus causes the temperature of the gas to increase immediately. Because of this, an expansion chamber operating in the usual manner is never really adiabatic in the sense that its temperature may be calculated from a volume expansion ratio. This compressive effect also causes the supersaturation

obtained by the expansion to decrease immediately so that the supersaturation is never constant.

4. THE CONTINUING EXPANSION TECHNIQUE. The technique devised in this laboratory at least partially overcomes this problem. A secondary valve is activated after the main expansion is completed. This valve continues the expansion, and its orifice is adjusted so that it just compensates for the compression due to boundary layer gas heating.[4,7] Thus, a small arbitrary volume of gas at the center of the chamber remains at the same pressure, volume, and temperature for an extended period until the slower effects of heat conduction and convection begin to warm the center of the chamber. This technique maintains a constant supersaturation at the center for about half a second[4] provided no dropwise condensation takes place.

5. ACCURACY IN MEASUREMENTS. Since we are now assured of a constant supersaturation, we are now justified in using one of the adiabatic laws to determine the degree of supersaturation from the pressure ratio. Allard[4] calculates supersaturations correct to two decimal places. He states that it is necessary to know temperature to 0.1 ^{o}C, γ to 0.0001 and pressure to 0.5 mm Hg in order to determine supersaturation with this accuracy.

6. SOURCES OF ERROR. There are still several possible sources of error which need to be studied before the accuracy of this determination of supersaturation is assured. Then accurate measurements of this homogeneous nucleation rate

versus supersaturation can be attempted. Allard[4] discusses possible errors.

It is necessary to maintain the top glass at a higher temperature than the liquid in order to prevent condensation on the top, which obscures vision, and in order to stabilize the gas mixture and damp out the convection currents. This causes an inhomogenity in the gas mixture, and the supersaturation attained after expansion is not perfectly uniform throughout the entire volume. It should also be mentioned that convection currents are a useful and necessary aid to reestablishing a state of saturation after the cycle is completed, that is after the chamber has been compressed back to its initial pressure. Diffusion of vapor is so slow a process, that if the convection currents are damped out too quickly, a state of saturation may not be attained during a reasonable waiting interval between expansions. Thus, a temperature gradient needs to be found which is high enough to prevent condensation on the top, but not high enough to cause appreciable uncertainty in the supersaturation; one which is high enough to damp out the convection currents before the next expansion, but not so high that the convection currents are damped out before a state of supersaturation is established.

It is also necessary to determine how long the supersaturation remains constant in the center when the continuing expansion technique is employed. That is, how long does it take for convection and conduction to reduce the supersat-

uration measureably? The calculation by Carstens[8] which was relied upon by Allard, is only an approximation and should be checked experimentally.

It is also desirable to test the validity of the adiabatic laws for determining supersaturation. It is possible that γ may be changing during the expansion since one of the constituents of the gas is a condensable vapor. In practice γ changes with both temperature and pressure for a real gas. This effect is small enough to be neglected in most experiments.

All sources of background caused by heterogeneous nucleation must be minimized or elimimated if possible. Various sources of background are dust, ions due to normal cosmic and terrestrial radiation, photonucleation due to short wave length components of illumination used in photography, and re-evaporation nuclei. Over the years, the first three sources mentioned have been studied and techniques developed to effectively eliminate them.[1,2,3] However, re-evaporation nuclei should be given further study.[4]

Finally, when the gas in the chamber is cooler than the surrounding walls, heat flows in from the walls. Thus, when the gas is compressed back to its initial pressure, it does not return to its initial temperature, but to some higher temperature. A similar problem exists with the temperature gradient. The heat which is pumped in is not distributed uniformly throughout the gas mixture, but the heated gas tends to rise to the top and causes a larger temperature gradient

also be allowed during the waiting interval for the static gradient to be reestablished. The time required for the bulk temperature and the temperature gradient to return to their initial states should be measured.

7. STATEMENT OF PROBLEM. It is the main purpose of this research to investigate the validity of using the adiabatic laws to determine the temperature from the pressure ratio. Some of the effects which might invalidate the use of the adiabatic laws will be studied. Special consideration will be given to the accurate calculation of γ.

Carstens' approximate calculation of the heat flow into the chamber due to conduction will be checked. A measurement will be made of how long the chamber remains adiabatic after an expansion when the continuing expansion technique is used. The static temperature gradient throughout the chamber will be measured to provide a knowledge of the initial temperature at any point in the chamber. Finally, a measurement will be made of how long it takes for the temperature and the temperature gradient to return to their initial values during the waiting interval.

It is not the purpose of this research to exhaustively investigate all possible sources of error in measuring homogeneous nucleation rates. Some of the other possible sources of error will be the subject of other investigations.

CHAPTER II

HOW A STATE OF SUPERSATURATION IS ACHIEVED

It is desirable to understand thermodynamically how a state of supersaturation is achieved in the cloud chamber so that an analysis of the errors in measuring the supersaturation can be made.

In its quiescent state the cloud chamber contains a non-condensable gas at pressure P_1, the temperature T_1, and volume V_1, which is saturated with a condensable vapor. The chamber is then suddenly adiabatically expanded. This causes the volume to increase to V_2, and the pressure and temperature to decrease to P_2 and T_2, according to the adiabatic law

$$T_1 P_1^{\frac{1-\gamma}{\gamma}} = T_2 P_2^{\frac{1-\gamma}{\gamma}}. \qquad (1)$$

Before expansion there is a mass of vapor m_1 present in the volume V_1 with a density m_1/V_1. This density, ρ_0, is called the saturation vapor density at T_1. Immediately after expansion, the original mass of vapor, m_1, will be distributed in the volume V_2. The new vapor density of the vapor is ρ_2. During the expansion, the vapor pressure decreases according to Eq. (1), but the saturation vapor pressure decreases by a larger amount. Fig. 1 demonstrates this result. In this figure, the equilibrium vapor pressure curve is drawn from data given in the International Critical Tables[9]. The excess vapor is therefore in a metastable state and would like to

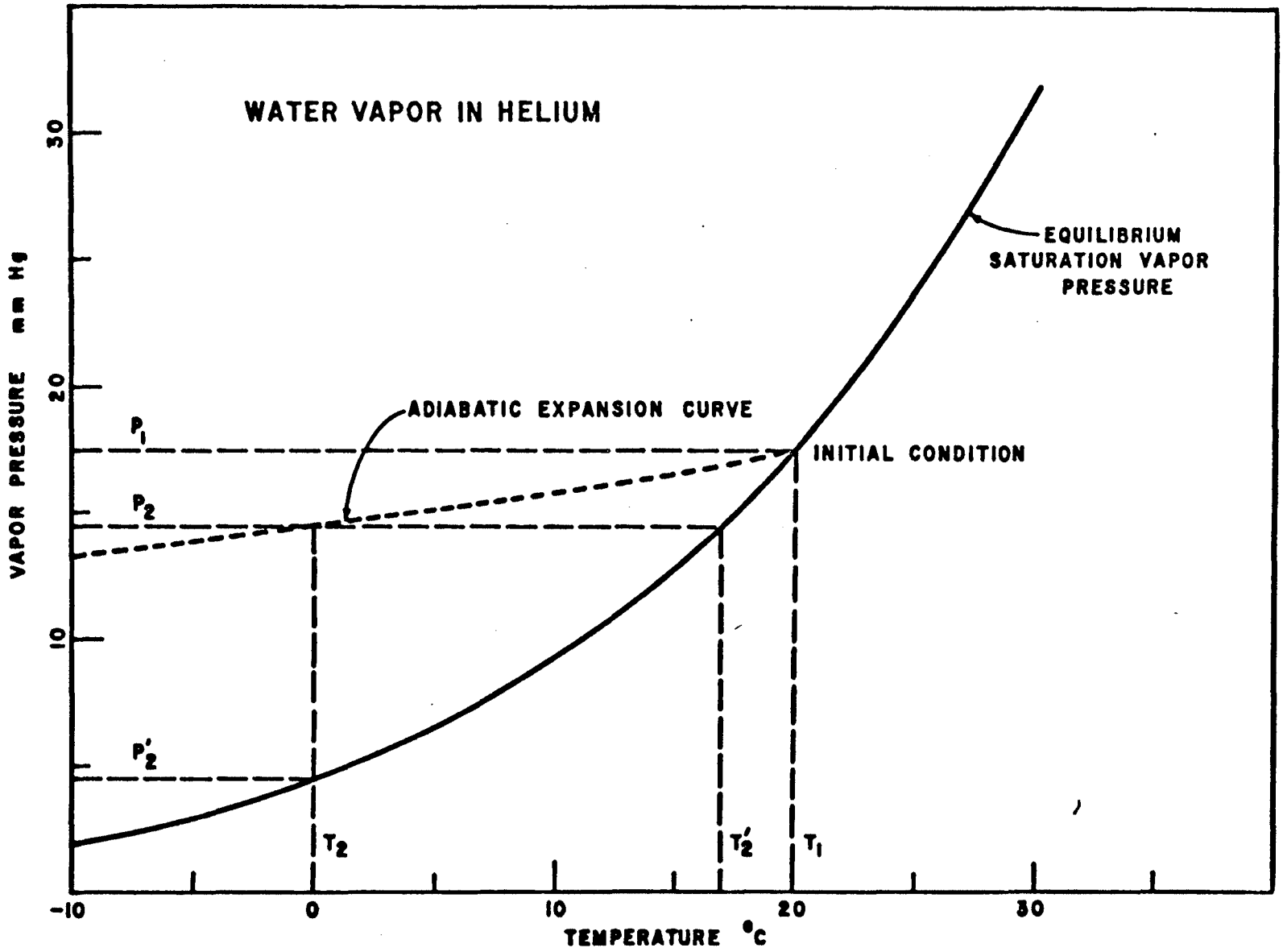
WATER VAPOR IN HELIUM
EQUILIBRIUM SATURATION VAPOR PRESSURE
ADIABATIC EXPANSION CURVE
INITIAL CONDITION
P_1
P_2
P'_2
T_2
T'_2
T_1
VAPOR PRESSURE mm Hg
TEMPERATURE °C
30
20
10
-10
0
10
20
30

FIG. 1

condense out of the inert gas. If the proper nuclei are present to initiate the phase change, the excess vapor will condense. The supersaturation is defined[10] by the ratio of the vapor density, ρ_2 to the saturation vapor density ρ_∞.

It should be noted that an equivalent definition of supersaturation is the ratio of the vapor pressure p_2 at T_2 to the saturation vapor pressure at T_2. This result easily follows from the perfect gas law. This equivalent definition was the one which Fig. 1 demonstrates.

Schmitt,[11] Dawbarn,[12] and Grayson[13] utilize this definition of supersaturation in their investigations. They can measure the initial total pressure P_1 and the initial temperature T_1. They then expand to a lower pressure P_2 which is measured. From the adiabatic law

$$T_2 = T_1 \left(\frac{P_1}{P_2}\right)^{\frac{1-\gamma}{\gamma}} \tag{2}$$

they calculate T_2. With this knowledge at hand, they look in the International Critical Tables[9] to find the saturation vapor pressure of water p_∞ at T_2. Once p_∞ is known, the vapor pressure after expansion can be easily determined from the fact that

$$p_2 = p_o \frac{P_2}{P_1}. \tag{3}$$

The supersaturation then is $p_2/p_\infty = S$

This is a time consuming procedure which must be repeated for every expansion. Since no way can be found to

calculate supersaturations without looking up vapor pressures in a table, the job has been given to the I.B.M. 1620 computer on this campus. The pertinent section of the International Critical Tables[9] has been fed into the computer's memory so that now the computer does the whole job of calculating supersaturations.

CHAPTER III

POSSIBLE ERRORS IN MEASURING SUPERSATURATIONS

Once the process of obtaining a state of supersaturation is understood thermodynamically, an attempt can be made to trace the sources of error in determining the supersaturation. When the sources of error are understood, steps can be taken to minimize them.

1. SUMMARY OF SOURCES OF ERROR. The only quantities which can be measured are the initial total pressure, P_1, the final total pressure, P_2, and the initial temperature, T_1. From these three quantities, all the other quantities necessary for a determination of p_2 and p_∞ can be calculated. Any errors in P_1, P_2, and T_1 will be propagated through the whole process of determining p_2 and p_∞ and will be reflected in value obtained for S. Let us analyze the process involved in determining S and note the sources of error at each step.

From T_1, the saturation vapor pressure for water must be determined from a table. Any error in T_1 will cause a corresponding error in the value obtained for p_0, the saturation vapor pressure prevailing initially. In addition, the presence of the helium above the water causes an increase in the vapor pressure of the water due to an effect analogous to osmotic pressure. This dependence of the vapor pressure on helium pressure has been neglected by Allard,[4] Schmitt,[11] Grayson,[13] and Dawbarn.[12]

It is important to know the vapor pressure accurately because the next quantity which must be determined is γ, the ratio of the specific heats, c_p/c_v, for the mixture of helium and water vapor. This quantity is needed to determine T_2 from

$$T_2 = T_1\left(\frac{P_1}{P_2}\right)^{\frac{1-\gamma}{\gamma}}. \qquad (2)$$

γ is dependent on temperature, pressure and the constituency of the gas mixture. Furthermore γ changes during the expansion since the gas mixture is not an ideal gas. The accurate determination of γ is one of the major obstacles to the accurate determination of T_2, the final temperature, and ultimately the supersaturation. It should also be mentioned that Eq. (2) is an equation which applies only to a perfect gas. A condensing vapor is far from being a perfect gas.

After T_2 is calculated, p_∞, the saturation vapor pressure at T_2 can be determined from a table. Again the error in T_2 is reflected in the value obtained for p_∞ and again this value will be raised because of the pressure of the helium on the water.

Finally, the errors in P_1 and P_2 cause an error in p_2 which is calculated using these quantities. The supersaturation is then in error according to the error in p_o and p_∞. Possibly some of the sources of error are negligible compared to others, but the above qualitative review of the possible errors serves to point out the many things which needed to be considered. These things will now be individually considered

in more detail.

2. ERROR IN THE EQUILIBRIUM VAPOR PRESSURE. The total pressures P_1 and P_2 can be measured to 0.1 mm Hg, and the initial temperature T_1 can be measured to 0.05°C. The change in the saturation vapor pressure at 22°C ± 0.05° is ± 0.062 mm Hg. The total vapor pressure is approximately 20 mm Hg at 22°C.

Before χ is calculated let us investigate the magnitude of the error caused by the vapor pressure raising due to the presence of the helium, since the error due to this effect may be negligible compared to the error due to the uncertainty in temperature.

During the quiescent state, the vapor in the cloud chamber is in equilibrium with the liquid water. The condition for equilibrium with the liquid water is[14]

$$\mu_v(T,p) = \mu_l(T,P), \tag{4}$$

where μ_v is the chemical potential of the vapor and μ_l is the chemical potential of the liquid. At constant temperature this equation implies that $p = f(P)$. Therefore, using the chain rule,

$$\left(\frac{\partial \mu_v}{\partial p}\right)_T \left(\frac{\partial p}{\partial P}\right)_T = \left(\frac{\partial \mu_l}{\partial P}\right)_T . \tag{5}$$

Since $\mu = G/n$ for a system of one component, the fundamental equation of Gibbs free energy,

$$dG = -SdT + VdP, \tag{6}$$

may be divided through by n to yield

$$d\mu = -\bar{S}dT + \bar{V}dP, \tag{7}$$

where $\overline{S}$ is the molar entropy and $\overline{V}$ is the molar volume. Assuming $\mu = \mu(P,T,)$, one may write

$$d\mu = \left(\frac{\partial \mu}{\partial T}\right)_P dT + \left(\frac{\partial \mu}{\partial T}\right)_T dP. \tag{8}$$

Equating the respective coefficients of dT and dP, one obtains

$$\left(\frac{\partial u}{\partial T}\right)_P = -\overline{S}, \tag{9}$$

and

$$\left(\frac{\partial u}{\partial P}\right)_T = \overline{V}. \tag{10}$$

Substituting Eq. (10) into Eq. (5)

$$\overline{V}_v\left(\frac{\partial p}{\partial P}\right)_T = \overline{V}_l, \tag{11}$$

or

$$\frac{\overline{V}_l}{\overline{V}_v} = \left(\frac{\partial p}{\partial P}\right)_T. \tag{12}$$

This is Gibbs' equation which gives the increase in vapor pressure due to an increase in total pressure. The constant $\overline{V}_l/\overline{V}_v$ is very small. As an estimate, the vapor occupies approximately 448,000 cc/mole at room temperature and 20 mm Hg pressure, and the liquid occupies only 18 cc/mole. Thus $\overline{V}_l/\overline{V}_v$ is approximately 0.00004. The total pressure is about 1330 mm Hg and as was implied above, the vapor pressure of water is about 20 mm Hg. This means that $P_g = (P-p)$ is a little over 1300. Assuming $\overline{V}_l/\overline{V}_v$ to be constant over the range of integration from P = 20 mm Hg to P = 1330 mm Hg, Eq. (12) becomes

$$\frac{\bar{V}_l}{\bar{V}_v}\int_{20}^{1330} \partial P \text{ const.T} = \int_{20}^{p} \partial p \text{ const.T} .$$

Integrating, one obtains (0.00004) (1330-20) = (p-20) or $\Delta p \approx 0.052$ mm Hg. This is on the same order of magnitude os the uncertainty of 0.062 mm Hg in the vapor pressure due to an uncertainty of 0.05°C in T.

Fortunately this error which has been neglected is constant and does not fluctuate as does the error due to the uncertainty of T_1, so the precision is still good.

3. THE ERROR IN γ. The error in γ due to the uncertainty in vapor pressure may now be calculated. This is done by utilizing the formula due to Richarz[15] for calculating the γ of a mixture of gases. This formula is

$$\frac{1}{\gamma-1} = \frac{1}{\gamma_g-1}\frac{p_g}{P} + \frac{1}{\gamma_v-1}\frac{p_v}{P}, \qquad (13)$$

where: γ is the composite ratio of the heat capacities for the mixture

γ_g refers in our situation, to the γ of He,

γ_v refers to the γ of water vapor,

p_g is the partial pressure of He,

p_v is the partial pressure of water,

P is the total pressure of the mixture.

In this equation P is the initial total pressure which is measured. The saturation vapor pressure, P_v, is found from tables. Thus p_g can be found from the difference between

P and p_v. This leaves as unknowns γ_v and γ_g. Schmitt[11] has devised a method for obtaining γ for water in the temperature range of interest. His method has the added advantage of determining not γ for a given termperature, but a mean γ over the temperature change which is produced by an adiabatic expansion. A brief summary of Schmitt's[11] method is given below.

On a large sheet of graph paper, isobaric curves of water vapor, in the temperature range of interest, are plotted on a temperature-entropy surface. The information necessary to do this comes from a table of thermodynamic properties of water.[16] Since reversible adiabatic processes are constant entropy processes, a constant entropy line is drawn at the proper entropy so that it intersects two isobars of interest (P_1 and P_2 of an expansion) at the temperatures of interest (T_1 and T_2 for the expansion). Since T_2 is not yet known; it must be estimated. This process causes little error in γ. Now that P_1 and P_2 are known for T_1 and T_2, Eq. (1) may be used in the form

$$\gamma = \left(1 \Big/ \left\{ \frac{\ln T_2/T_1}{\ln P_1/P_2} + 1 \right\}\right), \qquad (14)$$

to compute an average γ for that particular range of temperatures. This procedure is repeated for a variety of temperatures and then a curve is drawn of γ versus temperature for water.

Schmitt[11] accepted the standard textbook value of γ for helium which is 1.67. He then utilized Richarz's[15]

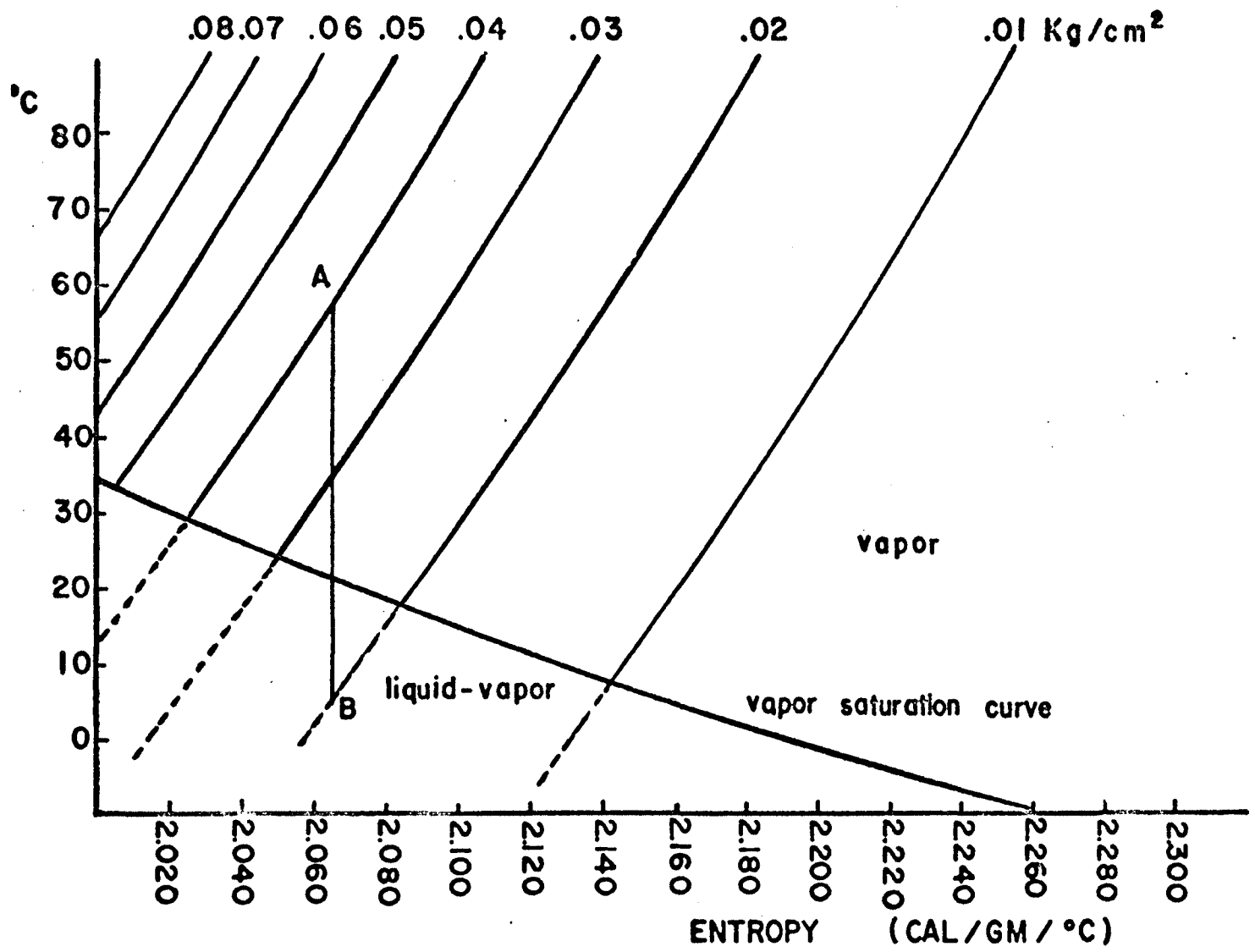
.08 .07 .06 .05 .04 .03 .02 .01 Kg/cm²
°C
80
70
60
50
40
30
20
10
0
A
B
liquid-vapor
vapor
vapor saturation curve
2.020
2.040
2.060
2.080
2.100
2.120
2.140
2.160
2.180
2.200
2.220
2.240
2.260
2.280
2.300
ENTROPY (CAL/GM/°C)

Fig. 2

formula to compute the γ for gas-vapor mixture at a given temperature and pressure from γ for helium and his γ for water vapor at that temperature. Before returning to the problem of the error in γ due to an error in the vapor pressure, additional comments need to be made concerning Schmitt's method.

Dawbarn[12] has used Schmitt's procedure to investigate γ for helium. The information necessary to do this came from a set of tables by Mann.[17] From this, Dawbarn found the γ for helium also varies significantly with temperature. A similar curve of γ versus temperature has been obtained for helium. Thus, Dawbarn uses his value of γ_g for helium at a given temperature and Schmitt's value of γ_v for water vapor and then utilizes Richarz's formula to determine the γ for the mixture for that temperature and pressure.

These efforts to obtain γ more accurately have a great deal of merit. As will be seen later, the supersaturation is very sensitive to an error in γ.

Very little information is available on the thermodynamic properties of helium at room temperature and atmospheric pressure. Since helium is such an important cryogenic material, most work on helium has been done at cryogenic temperatures. Available information on helium at room temperature and atmospheric pressure was accurate to only five percent.

The use of the adiabatic law, Eq. (1), is somewhat questionable, because this equation applies only to a perfect

gas. Admittedly, helium behaves nearly ideally. However, it fails to be perfect by a small but significant amount; a result which is reflected in Dawbarn's result that γ for helium varies significantly with temperature.

The situation is obviously even worse for a supersaturated vapor. The fact that the vapor condenses is very striking evidence that the vapor is not behaving as a perfect gas. This means that the use of Eq. (2), which is a law that applies only to a perfect gas where γ is constant, will lead to some error. This problem has been effectively obviated in the method devised by Schmitt.[11] Effectively, Eq. (2) becomes a semi-empirical equation, and the value of γ is adjusted so that the equation yields the correct final temperature for the range of temperatures and pressures of interest. The non-ideality of the gas has been taken into account in actual plots of the isobaric curves. Since the ideal adiabatic law is being used, this method therefore probably yields a value for γ which is not actually the ratio of the heat capacities, c_p/c_v. To illustrate, Dawbarn[12] obtains a value for γ for He of 1.6721 at 23.1°C and atmospheric pressure. On the other hand, Katz, Woods, and Leverton[18] obtained a value of γ of 1.6667 at 23.1°C and atmospheric pressure. They obtained an empirical equation for the γ of helium. This equation is

$$\gamma = 1.6669 - 0.0002P.$$

Thus γ for helium decreases with increasing pressure. Daw-

barn's[12] results, on the other hand, show γ for helium increasing with increasing pressure.

Now the problem of finding the error in γ due to all these effects can be considered. The formula due to Richarz[15] is

$$\frac{1}{\gamma-1} = \frac{1}{\gamma_g-1}\frac{p_g}{P} + \frac{1}{\gamma_v-1}\frac{p_v}{P}. \qquad (13)$$

Let us find the most probable error in $1/(\gamma-1)$ due to the standard deviation in all the other factors. The most probable error is

$$\triangle^2 = \triangle^2 p_v + \triangle^2 p_g + \triangle^2 P + \triangle^2 \gamma_v + \triangle^2 \gamma_g, \qquad (15)$$

Where: $\triangle$ is the most probable error

$$\triangle p_v = \frac{\partial\left(\frac{1}{\gamma-1}\right)}{\partial p_v}\delta p_v,$$

δ is the standard deviation,

$$\triangle p_g = \frac{\partial\left(\frac{1}{\gamma-1}\right)}{\partial p_g}\delta p_g,$$

$$\triangle P = \frac{\partial\left(\frac{1}{\gamma-1}\right)}{\partial P}\delta P,$$

$$\triangle \gamma_g = \frac{\partial\left(\frac{1}{\gamma-1}\right)}{\partial \gamma_g}\delta \gamma_g,$$

$$\triangle \gamma_v = \frac{\partial\left(\frac{1}{\gamma-1}\right)}{\partial \gamma_v} \delta \gamma_v .$$

From Eq. (13)

$$\triangle p_v = \frac{1}{\gamma_v - 1} \frac{1}{P} \delta p_v ,$$

$$\triangle p_g = \frac{1}{\gamma_g - 1} \frac{1}{P} \delta p_g ,$$

$$\triangle p = -\left(\frac{p_g}{\gamma_g - 1} + \frac{p_v}{\gamma_v - 1}\right) \frac{\delta p}{P^2} ,$$

$$\triangle \gamma_g = -\frac{p_g}{P} \frac{1}{(\gamma_g - 1)^2} \delta \gamma_g ,$$

$$\triangle \gamma_v = -\frac{p_v}{P} \frac{1}{(\gamma_v - 1)^2} \delta \gamma_v .$$

In the above: $\gamma_v = 1.3435$,

$\delta \gamma_v = 0.005$,

$\gamma_g = 1.6721$,

$\delta \gamma_g = 0.005$,

$P = 1330$ mm Hg,

$\delta P = 0.1$ mm Hg,

$p_v = 20$ mm Hg,

$\delta p_v = 0.06$ mmHg,

$p_g = 1310$ mm Hg,

$\delta p_g = 0.1$ mm Hg,

Using the above values the contributions to the error in $1/(\gamma-1)$ are:

$$\triangle p_v = 1.30 \times 10^{-4},$$

$$\triangle p_g = 1.12 \times 10^{-4},$$

$$\triangle P = 1.14 \times 10^{-4},$$

$$\triangle \gamma_v = 3.12 \times 10^{-4},$$

$$\triangle \gamma_g = 1.09 \times 10^{-2}.$$

Using these values in Eq. (15), the error in $1/(\gamma-1)$ is 1.095×10^{-2}. The error in $1/(\gamma-1)$ due to an error in γ is

$$1.095 \times 10^{-2} = \sqrt{\left[\frac{\partial}{\partial\gamma}\left(\frac{1}{\gamma-1}\right)\delta\gamma\right]^2} = \frac{1}{(\gamma-1)^2}\,\delta\gamma,$$

$$= \frac{1}{(0.65)^2}\,\delta\gamma.$$

Thus $\delta\gamma = 0.0046$.

The bulk of the error in γ is due to the uncertainty of γ_g. All of the other factors contribute negligible error.

4. THE ERROR IN FINAL TEMPERATURE. Now that the error in γ has been found, the error in the final temperature can be computed. Remembering Eq. (2)

$$T_2 = T_1\left(\frac{P_1}{P_2}\right)^{\frac{1-\gamma}{\gamma}},$$

the error in T_2 due to the error in T_1, P_1, P_2 and γ will now be computed.

$$\triangle T_1 = \left(\frac{P_1}{P_2}\right)^{\frac{1-\gamma}{\gamma}} \delta T_1,$$

$$\triangle P_1 = T_1 \left(\frac{1-\gamma}{\gamma}\right) \left(\frac{P_1}{P_2}\right)^{\frac{1-\gamma}{\gamma}} \left(P_1\right)^{-1} \delta P_1,$$

$$\triangle P_2 = T_1 \left(\frac{\gamma-1}{\gamma}\right) \left(\frac{1}{P_1}\right)^{\frac{\gamma-1}{\gamma}} \left(P_2\right)^{\frac{-1}{\gamma}} \delta P_2,$$

and

$$\triangle \gamma = T_1 \left(\frac{P_1}{P_2}\right)^{\frac{1-\gamma}{\gamma}} \ln\left(\frac{P_1}{P_2}\right) \left(\frac{-1}{\gamma^2}\right) \delta\gamma.$$

In these equations: $P_1 = 1330$ mm Hg,

$P_2 = 1008$ mm Hg,

$T_1 = 22^\circ C$,

$\gamma = 1.663$,

$\delta P_1 = 0.1$ mm Hg,

$\delta P_2 = 0.1$ mm Hg,

$\delta T_1 = 0.05^\circ C$

$\delta\gamma = 0.005$.

Using these values, the contributions to the error in T_2 are:

$\triangle T_1 = 0.0447^\circ K$,

$\triangle P_1 = 0.008^\circ K$,

$\triangle P_2 = 0.010^\circ K$,

$\triangle \gamma = 0.124^\circ K$.

Using these values in Eq. (15):

$$\delta T_2 = 0.133^\circ C.$$

5. THE ERROR IN THE SATURATION VAPOR PRESSURE AT T_2. From the International Critical Tables,[9] the vapor pressure of water p_∞, at $-5.25 \pm 0.133^\circ C$, is 2.768 ± 0.028 mm Hg. There is an uncertainty of 0.028 mm Hg in p_∞ at T_2.

6. THE UNCERTAINTY IN p_2. The vapor pressure after expansion, p_2, is given by

$$p_2 = p_o \left(\frac{P_2}{P_1}\right). \tag{16}$$

The errors due to p_o, p_2, and P_2 are:

$$\triangle p_o = \left(\frac{P_2}{P_1}\right) \delta p_o,$$

$$\triangle P_2 = \left(\frac{p_o}{P_1}\right) \delta P_2,$$

and

$$\triangle P_1 = -p_o \left(\frac{P_2}{P_1^2}\right) \delta P_1 .$$

Again, from previous sections:

$$P_1 = 1330 \text{ mm Hg},$$
$$P_2 = 1008 \text{ mm Hg},$$
$$p_o = 20 \text{ mm Hg},$$
$$\delta p_o = 0.062 \text{ mm Hg},$$
$$\delta P_2 = 0.05 \text{ mm Hg},$$
$$\delta P_1 = 0.05 \text{ mm Hg}.$$

Using these values, the contributions to the error in p_2 are:

$$\triangle p_o = 0.047 \text{ mm Hg},$$
$$\triangle P_1 = 1.5 \times 10^{-3} \text{ mm Hg},$$

and

$$\triangle P_2 = 1.13 \times 10^{-3} \text{ mm Hg}.$$

Thus the bulk of the error in p_2 is due to the error in p_o. It is important to know this factor very accurately. The error due to the other two factors is completely negligible.

Using the above values in Eq. (15), the error in p_2 is 0.049 mm Hg. The greater the ratio P_1/P_2, the more the error in p_o will be demagnified in p_2.

7. THE ERROR IN SUPERSATURATION. Now all the information necessary to calculate the error in S has been obtained. It will be remembered that $S = p_2/p_\infty$. The contributions to the error in S are:

$$\triangle p_2 = \frac{1}{p} \delta p_2,$$

and

$$\triangle p_\infty = -p_2/p^2 \ \delta p \ .$$

In the above:

$$p_2 = 15.0 \text{ mm Hg},$$

$$p_\infty = 2.768 \text{ mm Hg},$$

$$\delta p_2 = 0.047 \text{ mm Hg},$$

and

$$\delta p_\infty = 0.028 \text{ mm Hg}.$$

Using the above values the contributions to the error in S are:

$$\triangle p_2 = 0.017,$$

and

$$\triangle p_\infty = 0.0548.$$

The error in S due to these factors is 0.057.

The above analysis was performed for a supersaturation of 5.42. This is a fairly high value so the analysis was repeated for supersaturations of 4.9 and 1.6. The latter supersaturation is too small to cause homogeneous nucleation.

Table I

How Obtained	Quantities	Value	Deviation	Main Cause of Error
Measured Quantities	P_1	1330.0 mmHg	$\pm$0.1 mmHg	
	P_2	1008.0 mmHg	$\pm$0.1 mmHg	
	T_1	22.00°C	$\pm$0.05°C	
From Table	p_0	19.872 mmHg	$\pm$0.062 mmHg	T_1
$P_1 - p_0$	p_g	1310 mmHg	$\pm$0.1 mmHg	P_1
Schmitt's Method	γ_v	1.344	$\pm$0.005	Curves could not be plotted more accurately.
	γ_g	1.672	$\pm$0.005	
Richarz's Formula	γ	1.663	$\pm$0.005	γ_g
$T_2=T_1\left(\frac{P_1}{P_2}\right)^{\frac{1-\gamma}{\gamma}}$	T_2	-5.25°C	$\pm$0.13°C	γ
From Table	P	2.768 mmHg	$\pm$0.028 mmHg	T_2
$p_2 = p_1\left(\frac{P_2}{P_1}\right)$	p_2	15.0 mmHg	$\pm$0.05	p_0
$S = \left(\frac{p_2}{p}\right)$	S	5.42	$\pm$0.057	p_∞

An error analysis was performed at that value only to find how Δ varies as S varies. At S = 4.9, the error was $\pm$ 0.06 and at S = 1.6 the error was $\pm$ 0.02. Apparently in the range of interest in this laboratory, S = 4.0 and above, the error in the supersaturation is around 0.06. It seems that Allard[4] was in error when he states that he knew S correct to two decimal places.

8. THE ERROR IN THE NUCLEATION RATE. A complete error analysis of the nucleation rate would be an extremely difficult procedure. There is so much disagreement between the various theories that the results of the analysis would not be very meaningful once they were obtained.

As an estimate of how much error in the nucleation rate an error in supersaturation causes, the above results were applied to the Becker-Döring theory. This theory was chosen because its results lie about in the middle of the range of values predicted by the various theories.

Grayson[13] has computed the nucleation rates versus supersaturation predicted by the various theories and has displayed the results on a graph. By referring to this graph, it was found that at S = 5.40 $\pm$ 0.057 the nucleation rate was $6 \times 10^{5} \pm 5 \times 10^{5}$. The error at other levels of supersaturation caused by an uncertainty of 0.06 in S, was also about 100%.

This drastic error is caused almost entirely by the error in γ of helium. The error in the initial temperature also makes a much smaller but still significant contribution

to the error in the nucleation rate. The pressures are presently being measured with sufficient precision that they cause negligible error. Since this laboratory is presently engaged in trying to obtain an empirical nucleation rate law for water it is important that some means be found of obtaining γ for helium more accurately.

CHAPTER IV

THE EXPERIMENTAL APPARATUS

A complete description of the cloud chamber facility is given by Allard[4] so only a general description of the apparatus will be given here with the inclusion of some details about the pressure and volume circuits.

1. THE CLOUD CHAMBER. A drawing of the cloud chamber is shown in Fig. 3. As can be seen, the cloud chamber consists of two airtight volumes separated by a rubber diaphragm. The position of this diaphragm is controlled by adjusting the air pressure in the lower volume. The flow of air in and out of the lower volume is regulated by a series of electronically controlled solenoid valves.

The upper volume is the one in which measurements are made. It is enclosed by a pyrex cylinder on the side and a 3/4 inch glass plate on the top. These glass surfaces allow visual and photographic observation of the droplets formed in the chamber. These is a hole in the pyrex cylinder in which a pressure transducer is mounted. Another hole has been drilled in the glass cylinder through which a thermocouple is placed.

The upper volume is filled with 99.99% pure helium. The rubber diaphragm is covered with water to a depth of several inches. This water serves to saturate the helium above it, and to trap any dust particles which might be introduced into

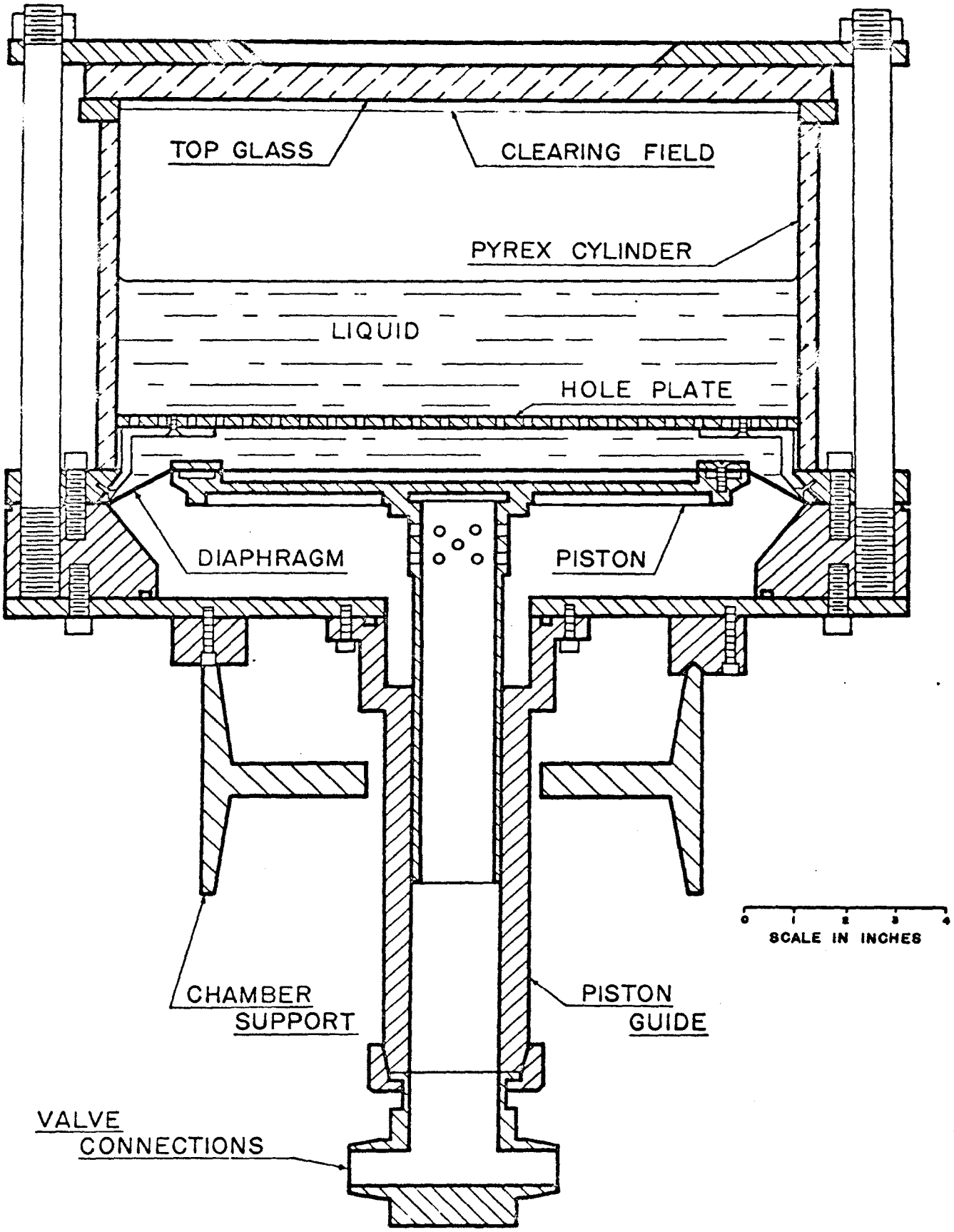

THE CLOUD CHAMBER

Fig. 3

the upper volume.

The rubber diaphragm is attached to a large aluminum piston plate which in turn is attached to a guide cylinder which slides up and down in a piston guide. The lower end of the piston guide is threaded to accept a coupling from a manifold where the valves are located. Holes have been drilled in the guide cylinder to allow air to flow into and out of the lower volume.

Attached to the aluminum piston plate is a brass rod which is connected to the wiper arm of a linear potentiometer. This potentiometer serves as a volume transducer.

2. THE VOLUME TRANSDUCER SYSTEM. A block diagram of the volume transducer system is given in Fig. 4. Referring to this figure, the transducer power supply is a Systems Research Corporation, Model 3508C strain gauge power supply. This power supply is a highly isolated and regulated transistorized unit producing 0-30VDC up to 100ma. Its output voltage is constant to 0.01% with a variation of 95-135 VAC input. Its regulation is 0.01% from no load to full load. It has a ripple of only 0.05 mv rms. The primary of the power transformer is highly shielded from the secondary so that noise on the power line does not get into the output of the power supply.

This power supply feeds a linear potentiometer which was designed in this laboratory. The voltage across the potentiometer is maintained at 0.3 VDC. A basic diagram of the

VOLUME TRANSDUCER SYSTEM

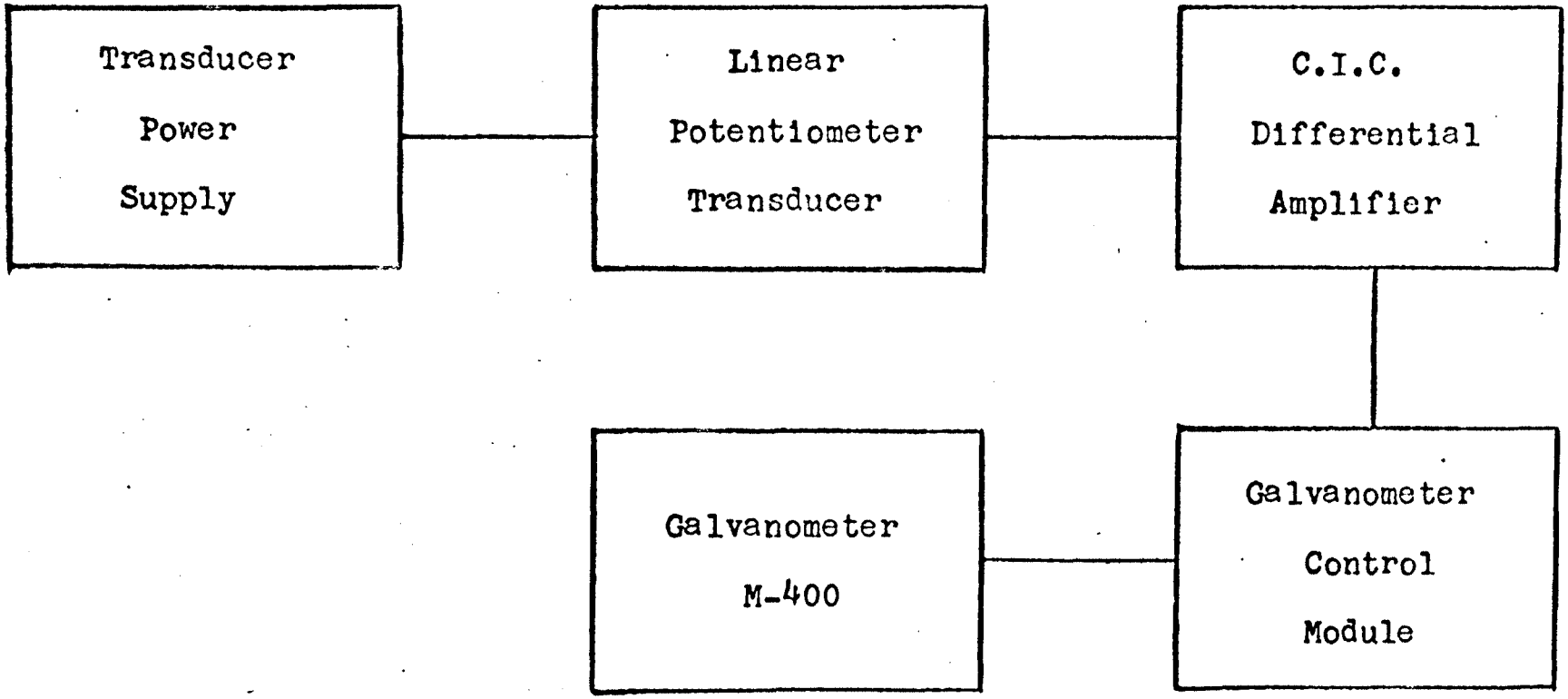

Fig. 4

linear potentiometer circuit is given in Fig. 5. The wiper arms of the transducer are operated by a push rod which is attached to the bottom of the piston plate. The transducer is designed so that the load on the input of the amplifier is constant.

The output of the volume transducer is fed to a California Instruments Corporation Model 3101B wideband DC amplifier. This amplifier is completely transistorized and is designed so that it may be used either as a single ended or a differential input amplifier. The mode of operation is determined by the plug-in attenuator used in the input of the amplifier. The model D3PB plug-in attenuator, which provided for differential input, was used in the volume transducer system. The differential input was chosen because it gave a lower noise level than the single ended mode of operation.

The amplifier gain was set 20 X. The amplifier has a very stable gain factor. This is accomplished by providing enough negative feedback so that the DC gain is reduced from 10^{9} X to a maximum of 10^{3} X.

The output of the amplifier is then fed to a Systems Research Corporation, Model 304E, galvanometer control module. This unit allows the signal to be attenuated and biased. The unit came equipped with 5% carbon resistors in the attenuation circuits. These were replaced by low thermal coefficient 1% resistors to eliminate drift. The bias was set so that the volume trace on the recording galvanometer was near the left hand edge of the recording paper. An attenuation

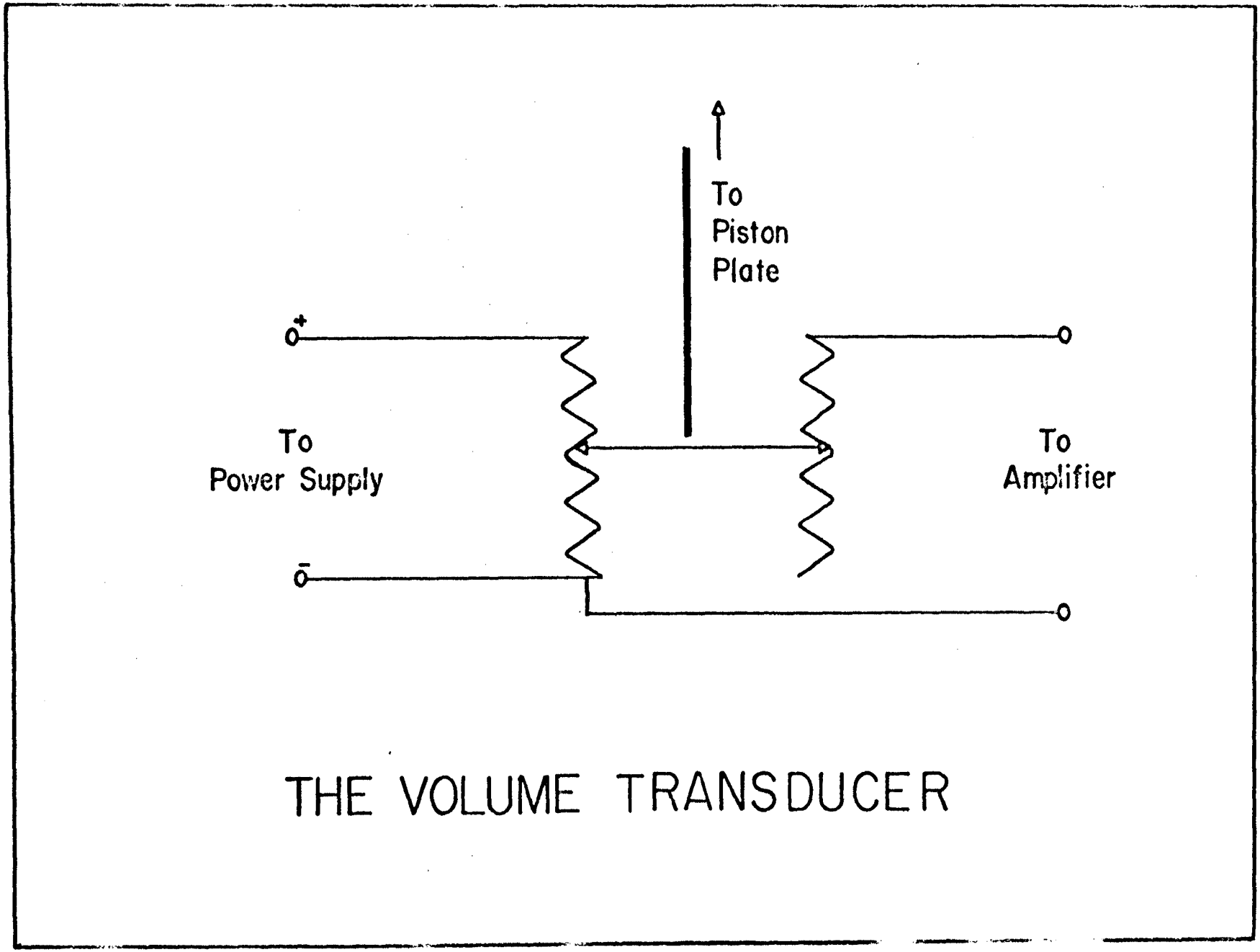
To
Piston
Plate
To
Power Supply
To
Amplifier
THE VOLUME TRANSDUCER

Fig. 5

was selected so that the volume trace did not go off scale during the operation of the cloud chamber. The proper attenuation was 120 ohms.

The signal from the galvanometer control module is then fed to a Honeywell, Model 1508, Visicorder with a model M-400 galvanometer. The Visicorder is a rack-mounted, direct-recording oscillograph which will simultaneously record up to 24 channels of data from DC to 5000 cycles per second. Light from an ultraviolet lamp reflects from mirrors on the galvanometers and exposes a light sensitive recorder paper. The image on the paper can be seen immediately by exposing it to room light and allowing the paper to photolize. The photolized image will eventually disappear. A permanent record may be taken by shielding the paper from room light and processing it in developing chemicals.

3. THE PRESSURE TRANSDUCER SYSTEM. The pressure is monitored by a Micro Systems, Incorporated, pressure transducerducer, Type P03BA5-50. This transducer has an operating range of 0-50psi. The transducer consists of four solid state elements arranged in a Wheatstone bridge. Strains caused in the solid state elements due to the flexing of the diaphragm on which they are fastened are converted into an electrical signal of 0.607 volts per 50psi.

The voltage to the transducer is supplied by another Systems Research Corporation, Model 3508C, power supply as described above. The power supply is adjusted to 5.00 volts. The transducer driver, furnished by the company, is not used.

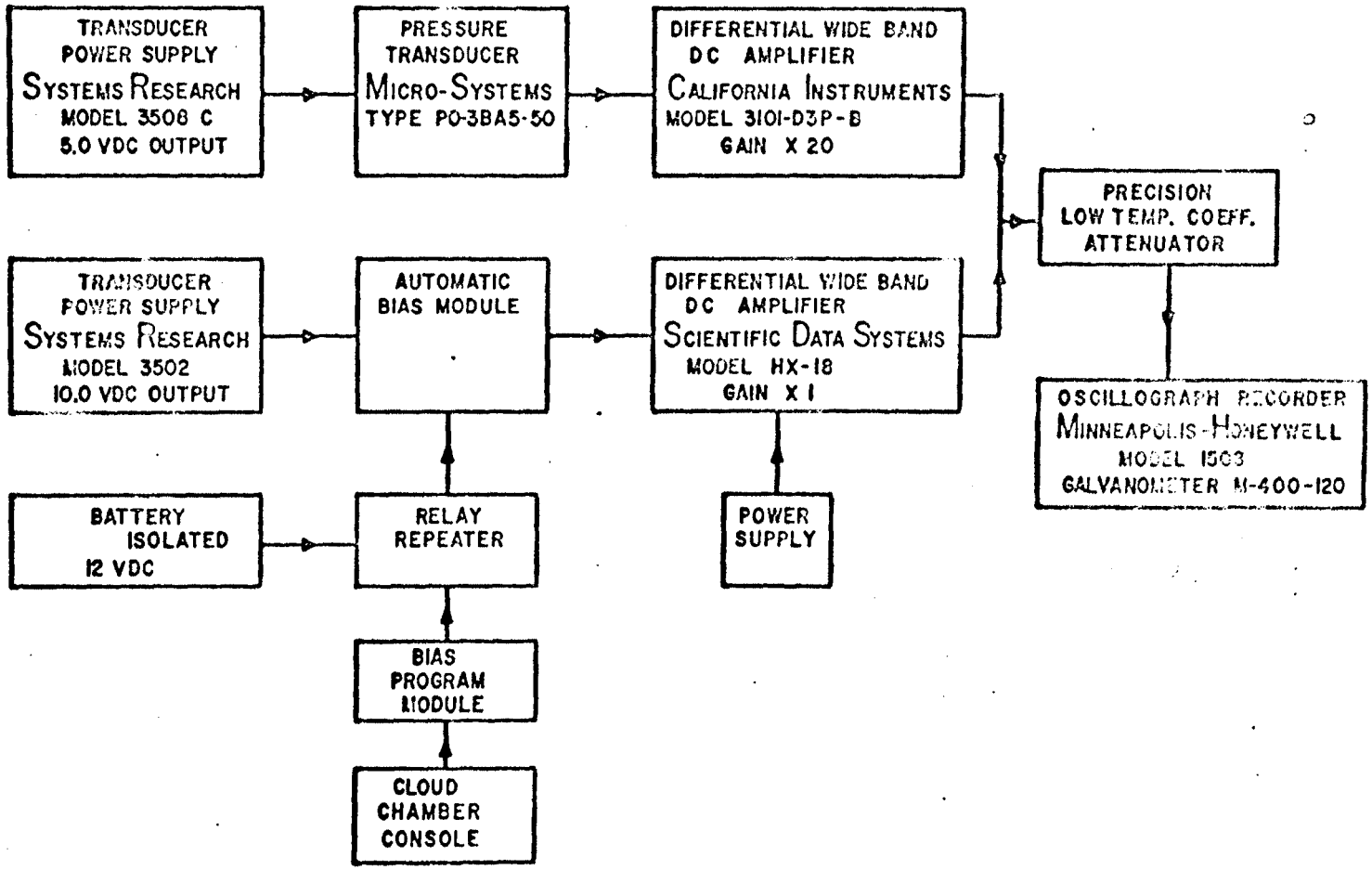
TRANSDUCER
POWER SUPPLY
SYSTEMS RESEARCH
MODEL 3508 C
5.0 VDC OUTPUT
PRESSURE
TRANSDUCER
MICRO-SYSTEMS
TYPE PO-3BA5-50
DIFFERENTIAL WIDE BAND
DC AMPLIFIER
CALIFORNIA INSTRUMENTS
MODEL 3101-D3P-B
GAIN X 20
PRECISION
LOW TEMP. COEFF.
ATTENUATOR
TRANSDUCER
POWER SUPPLY
SYSTEMS RESEARCH
MODEL 3502
10.0 VDC OUTPUT
AUTOMATIC
BIAS MODULE
DIFFERENTIAL WIDE BAND
DC AMPLIFIER
SCIENTIFIC DATA SYSTEMS
MODEL HX-18
GAIN X 1
OSCILLOGRAPH RECORDER
MINNEAPOLIS-HONEYWELL
MODEL 1503
GALVANOMETER M-400-120
BATTERY
ISOLATED
12 VDC
RELAY
REPEATER
POWER
SUPPLY
BIAS
PROGRAM
MODULE
CLOUD
CHAMBER
CONSOLE

Fig. 6

The output from the pressure transducer is amplified by another California Instruments Corporation, Model 3101B DC amplifier with the D3PB plug-in attenuation module for differential input operation. The gain of the amplifier is set at 20 X.

The output from the amplifier is fed to another channel of the Systems Research Corporation, Model 304E, galvanometer control module. The precision, low temperature coefficient capabilities of the attenuator is utilized, but it was found that the biasing capabilities of the module were inadequate for use in the pressure system. A separate, rather complex, biasing unit was designed in this laboratory and it is used to bias the pressure signal for proper display on the Visicorder. This biasing unit will be described in a later section.

After the signal has been properly attenuated and biased, it is displayed on another channel of the Honeywell, Model 1508, Visicorder for display.

4. THE AUTOMATIC PRESSURE BIAS SYSTEM. As was indicated in the discussion of errors, the pressure measuring system needs to have sufficient resolution that a pressure difference of 0.1 mm Hg can be detected. However, an expansion sufficient to cause nucleation causes a pressure drop of over 300 mm Hg. If the amplification of the pressure signal were sufficient to cause only a full scale deflection over this pressure change, a deviation of 0.1 mm Hg could not be detected at all. The resolution would be about ten

THE BIAS PROGRAM MODULE

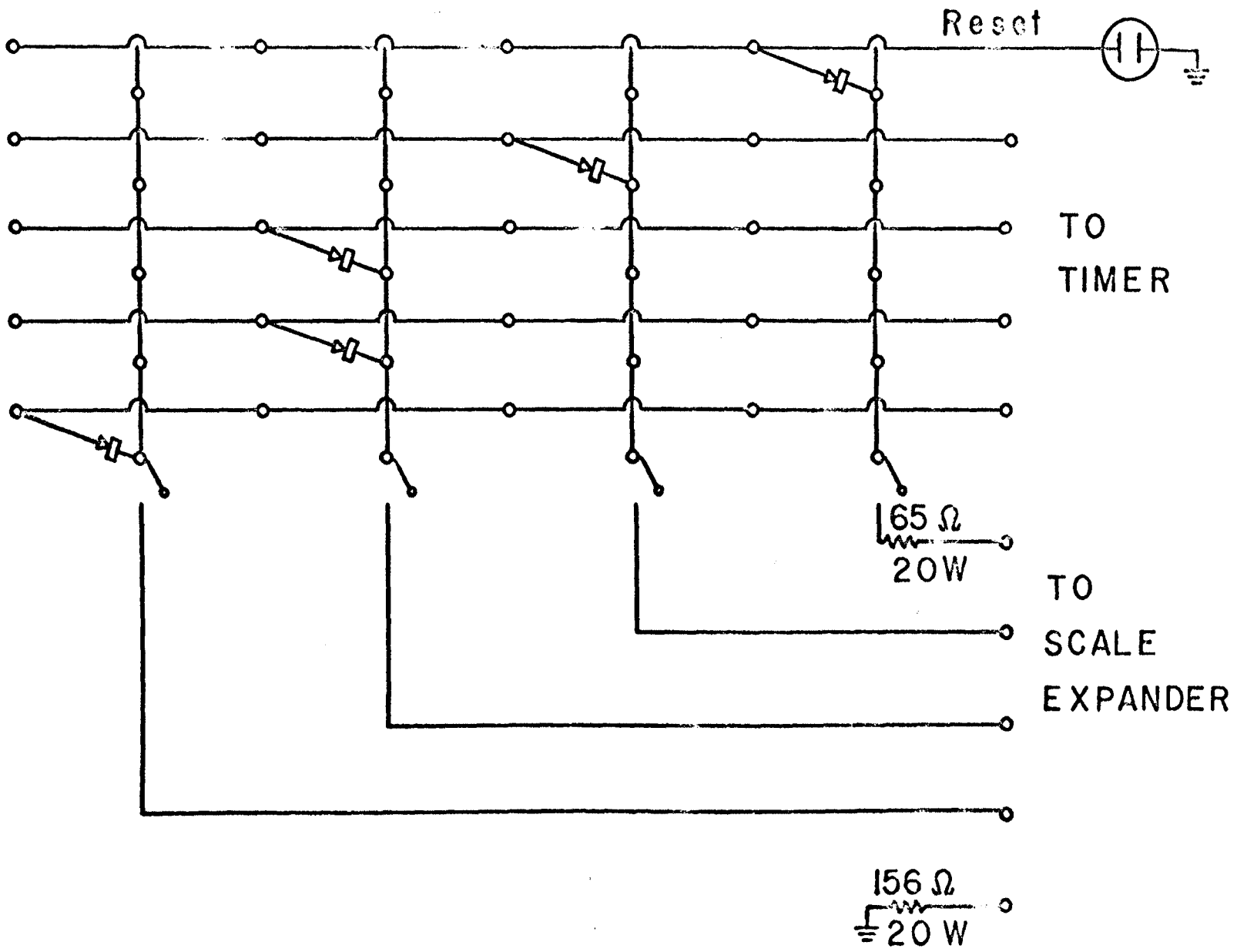

Fig. 7

times as coarse. On the other hand, if sufficient amplification were given to the pressure signal that the desired resolution were achieved, the trace deflection would far exceed the full scale capabilities of the recorder, and the galvanometer would be permanently damaged.

The solution to the problem was to design a biasing system which would automatically change its bias during the cloud chamber cycle so that a high gain could be given to the pressure signal and yet, the pressure trace would stay on scale and galvanometers would be protected.

The heart of the system to achieve the above described operation is the automatic bias module. This is a high precision bias unit with four channels which may be switched in and out at will. The bias voltage comes from a Systems Research Corporation Model 3502 power supply. The voltage is further regulated by temperature compensated, 9 volt, Zenor diodes in each channel. The 9 volts are fed through a reversing switch and placed across a precision Helipot, 100 ohm, 10 turn, linear potentiometer. Any desired voltage may be selected with this Helipot. The output from each Helipot is placed on the contacts of a C. P. Clare mercury wetted relay. There is a relay for each channel. When it is desired to utilize the bias furnished by a given channel, the relay for that channel is activated.

The voltage which is activated by a relay is fed through a Scientific Data Systems, Model HX-18 wideband differential amplifier with a gain of 1 X. This amplifier serves to lower

output impedance to 0.01 ohm so that the output impedance of the bias unit is independent of the potentiometer setting and the gain of the pressure signal is not affected by changing the bias. The signal from the operational amplifier is then used to bias the pressure signal.

The automatic bias module is switched from channel to channel, that is, from bias to bias, by a bias program module. The operation of this unit is as follows.

A signal is taken from the thyratron control timers which operate the various valves. For instance, a signal is taken when the chamber is in its quiescent state in order to find the initial pressure. When the chamber expands, this signal shuts off, and no signal is taken during the expansion. A signal is then taken from the timer which operates the continuing expansion valve. This signal causes the final pressure to be displayed. This process continues for all the pressure intervals of interest.

These signals from the thyratron control timers are passed through a diode array, designed by the author, in the bias program module. This array automatically sends the signals to the proper channel of the automatic bias module.

These signals do not pass directly to the automatic bias module, but are isolated from it by the relay repeater. The signals from the diode array activate a set of C. P. Clare mercury wetted relays. These relays then switch a voltage from a 12 volt battery to operate the relays in the automatic bias module. A battery is used to supply the

voltage to the relays in the automatic bias module because the voltage from the thyratron control timers is so noisy that it causes a great deal of noise in the pressure trace if it is placed directly on the automatic bias control module relays.

5. THE TEMPERATURE MEASURING SYSTEM. The temperature in the cloud chamber is measured by a 0.0005 inch diameter chromel-alumel thermocouple. Larger diameter thermocouples were first tried, but it was found that they had such a large heat capacity that they did not adequately respond to the temperature. A drawing of a thermocouple system which finally worked properly is shown in Fig. 8.

A chromel-alumel junction of 0.0005 inch wire is placed at the center of the chamber. This wire is stretched out and the chromel wire was spotwelded to a support of 0.006 inch chromel wire and alumel was spotwelded to the same size alumel wire. These support wires were then passed through tiny stainless steel tubes made from a hypodermic needle. The tubes pass through a teflon plug which is inserted in a quarter inch stainless steel tube. The stainless steel tube passes through an "O" ring seal fitting in the wall of the cloud chamber cylinder. The support wires were insulated and passed through the quarter inch tube and connected to two tiny wires from a shielded phono pick-up arm cable (Beldon # 8429-25). The electrical contacts were made with low thermal coefficient solder. These two junctions were then electrically insulated from each other and placed in an oil

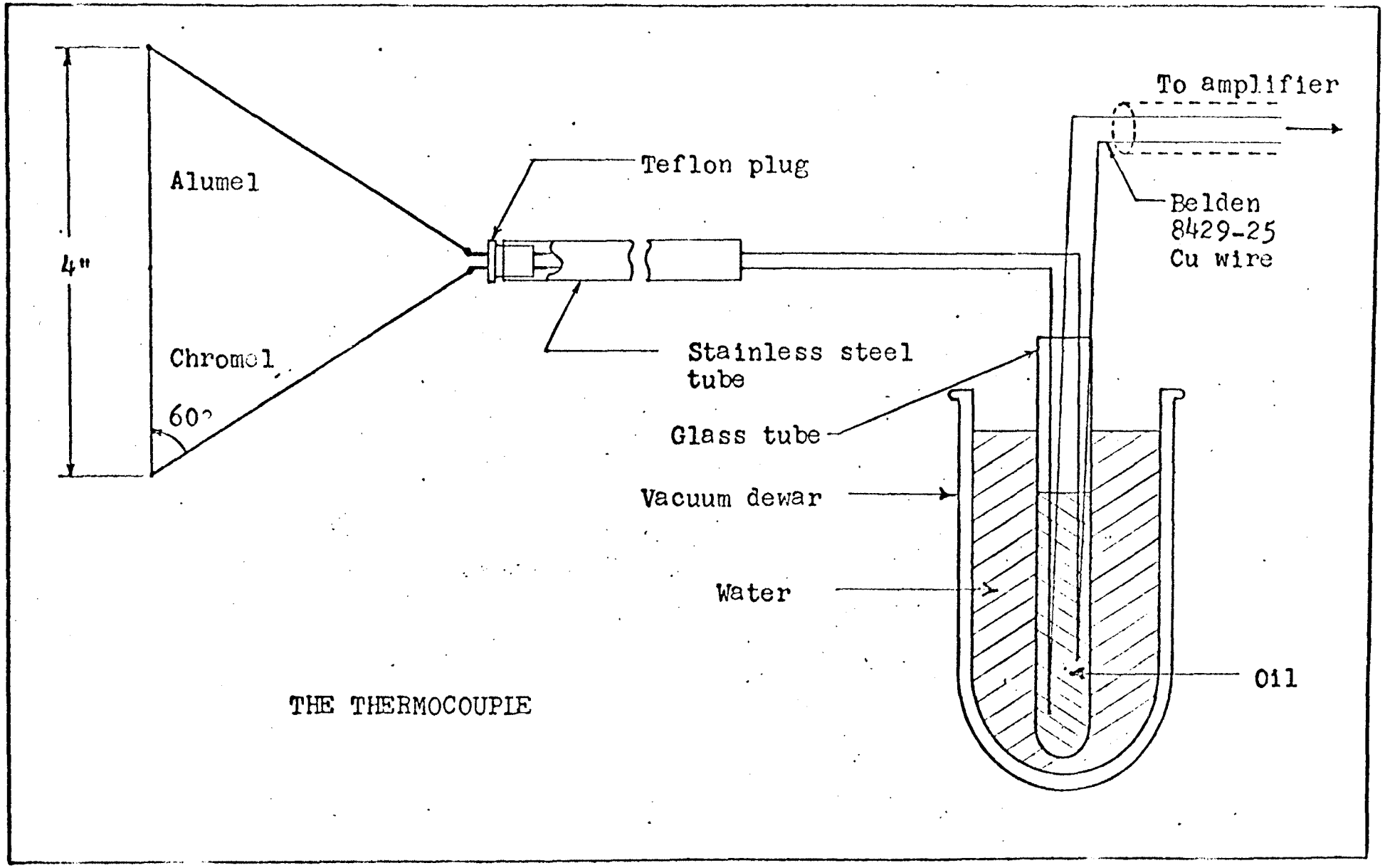
4"
Alumel
Chromel
60°
Teflon plug
Stainless steel tube
Glass tube
Vacuum dewar
Water
To amplifier
Belden 8429-25 Cu wire
Oil
THE THERMOCOUPLE

Fig. 8

bath in a small glass tube with its end sealed. This glass tube was then placed in a constant temperature water bath to assure that both junctions would be at the same temperature so that they could cause no thermoelectric potential.

The signal from the thermocouple is amplified by a California Instruments Corporation, Model 3101 B amplifier with the D3PB plug in attenuator module for differential input. The gain of the amplifier was set at 100 X. The signal from the amplifier was fed to a third channel on the Systems Research galvanometer control module. An attenuation of 180 ohms was used for the measurements.

It should be mentioned that during the experiments to be described below all the amplifiers were used in their differential input mode. After these experiments were completed, the signal cables were doubly shielded. After this was done, the lowest noise resulted from using the amplifiers in their potentiometric mode.

CHAPTER V

EXPERIMENTAL PROCEDURES AND RESULTS

1. STATIC TEMPERATURE MEASUREMENTS. It seems desirable to begin an experimental study of the thermodynamic properties of the cloud chamber by determining the steady-state temperature distribution in the sensitive volume of the expansion chamber. The chamber was inoperative throughout these measurements, the liquid level remaining in the fully expanded position. The chamber was not pressurized at this time. A temperature gradient was artificially imposed on the sensitive volume by means of a small electric heater located in the top of the cloud chamber enclosure. The power to the heater was adjustable and a temperature difference of $1^{\circ}C$ or less was maintained between the top glass and the liquid. It is the temperature distribution produced by this top-bottom temperature difference and the perturbations due to the walls which is to be determined. The top-bottom temperature difference was measured with an iron-constantin thermocouple. The "hot" junction was taped to the outside of the top glass and cold, or reference, junction was taped to the glass wall of the chamber below the liquid level.

Two theoretical calculations of the temperature distribution were made using the usual diffusion equation with suitable symmetry and simplified boundary conditions. The gas-vapor mixture in the sensitive volume is treated in the

BOUNDARIES FOR FIRST CALCULATION

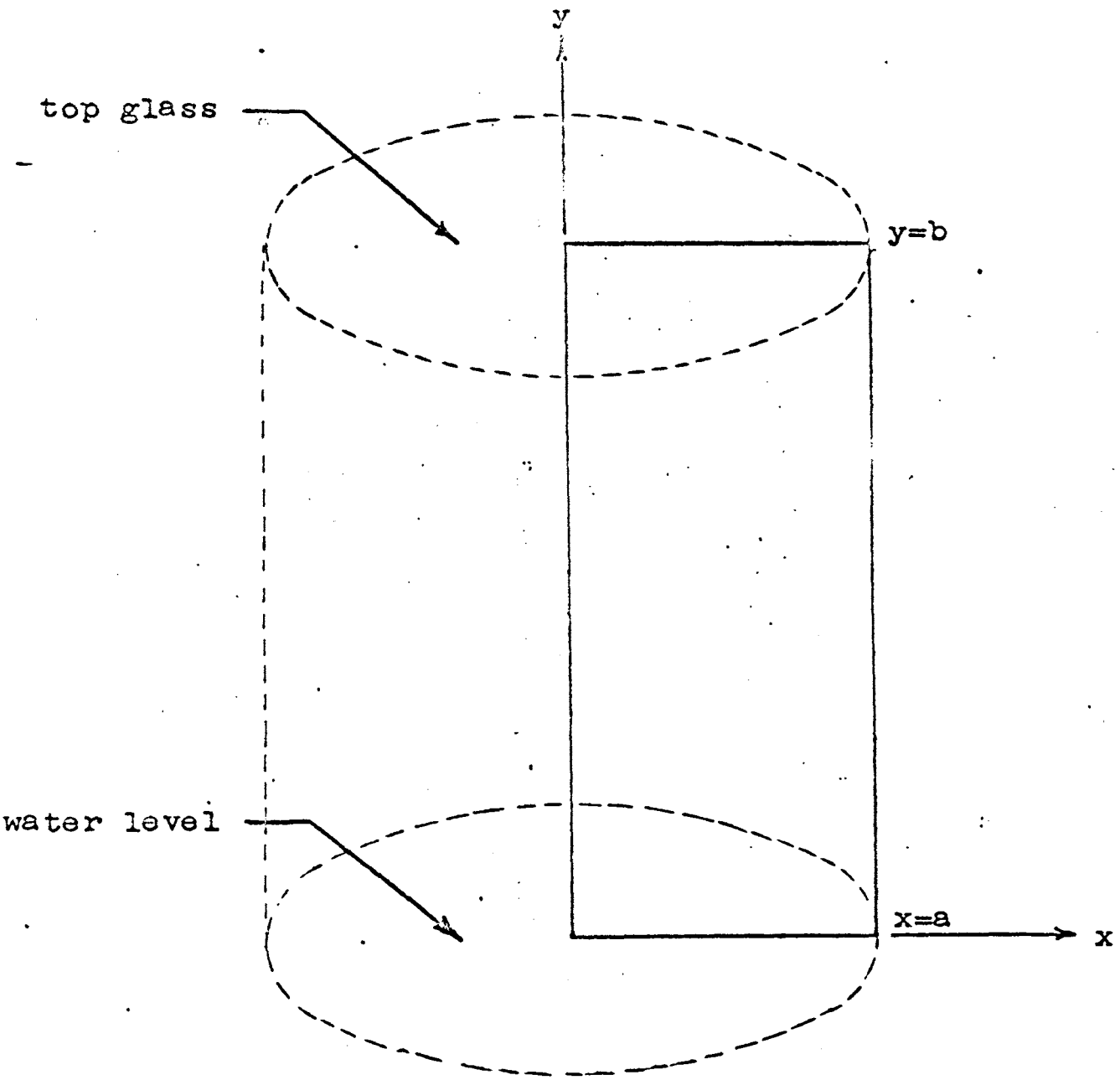

Fig. 9

steady state as a homogeneous solid. Since convection and radiation effects should be unimportant, the top, being warmer than the bottom, they were neglected throughout these calculations.

The first calculation was made for a homogeneous slab with the thermal constants of the gas. In effect it was assumed that the temperature distribution is symmetric with respect to the axis of the chamber. No attempt was made to estimate the effect due to the thermocouple probes. Therefore any plane which contains the axis will possess a temperature distribution characteristic of the entire chamber, see Fig. 9.

$$\frac{\partial^2 u}{\partial x^2} + \frac{\partial^2 u}{\partial y^2} = 0$$

$$u(0,y) = 0 \qquad 0 \leq y \leq b$$
$$u(x,0) = 0 \qquad 0 \leq x \leq a$$
$$u(a,y) = 0$$
$$u(x,b) = T.$$

The solution is

$$u(x,y) = \sum_{n=1}^{\infty} \left\{ \frac{4T}{(2n-1)\pi \sinh\left[\frac{(2n-1)\pi b}{a}\right]} \right\} \sin\left[\frac{(2n-1)\pi x}{a}\right] \sin\left[\frac{(2n-1)\pi y}{b}\right]$$

The first ten terms were evaluated using the computer for the conditions $T = 1^{\circ}C$, $a = 17$ cm, and $h = 11$ cm, the approximate conditions for the cloud chamber. The results are shown in Fig. 10.

The second calculation was made using cylindrical symmetry and the following boundary conditions:

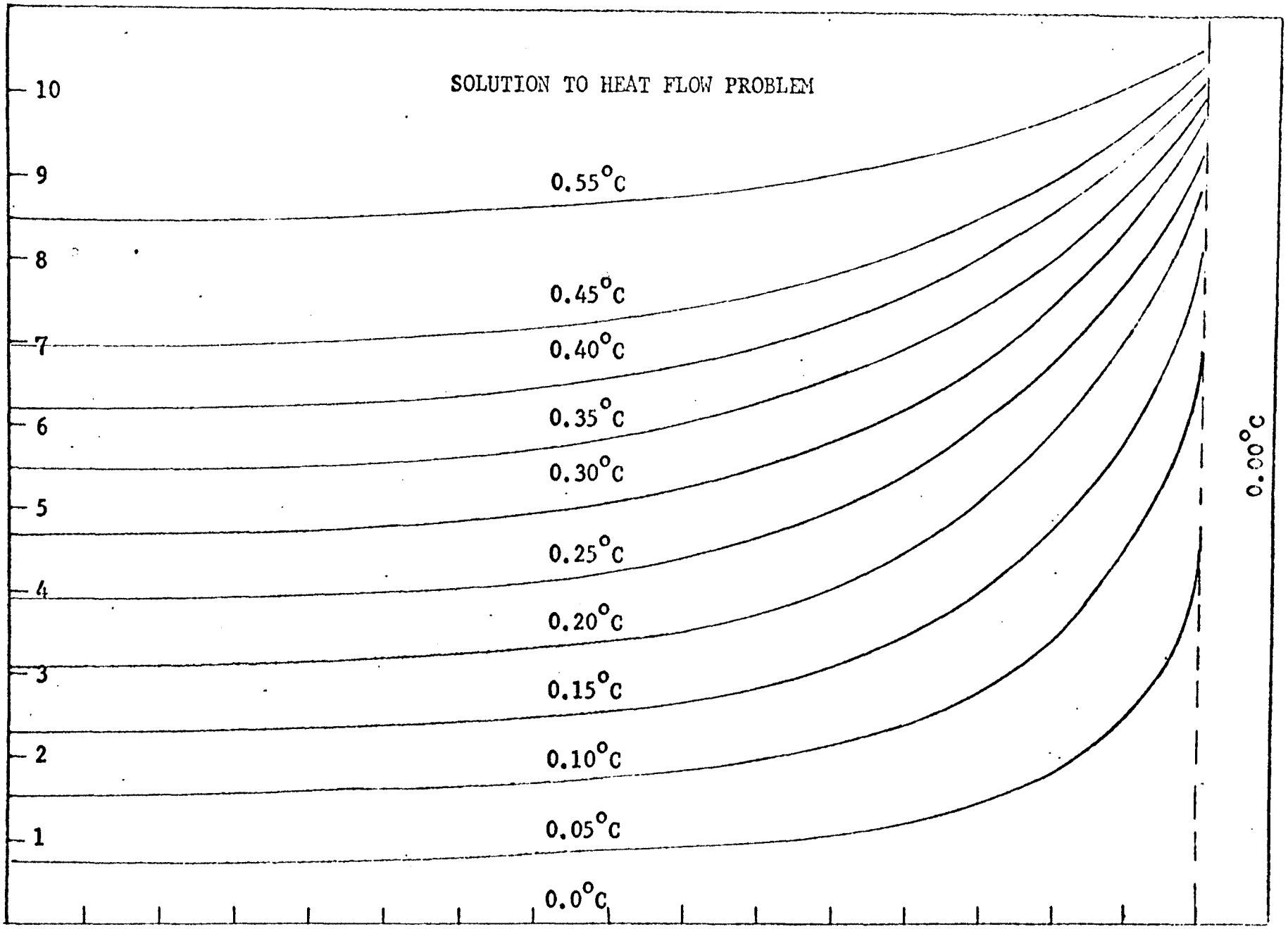
SOLUTION TO HEAT FLOW PROBLEM
10
9
8
7
6
5
4
3
2
1
0.55°C
0.45°C
0.40°C
0.35°C
0.30°C
0.25°C
0.20°C
0.15°C
0.10°C
0.05°C
0.0°C
0.00°C
0
2
4
6
8
10
12
14
16

Fig. 10

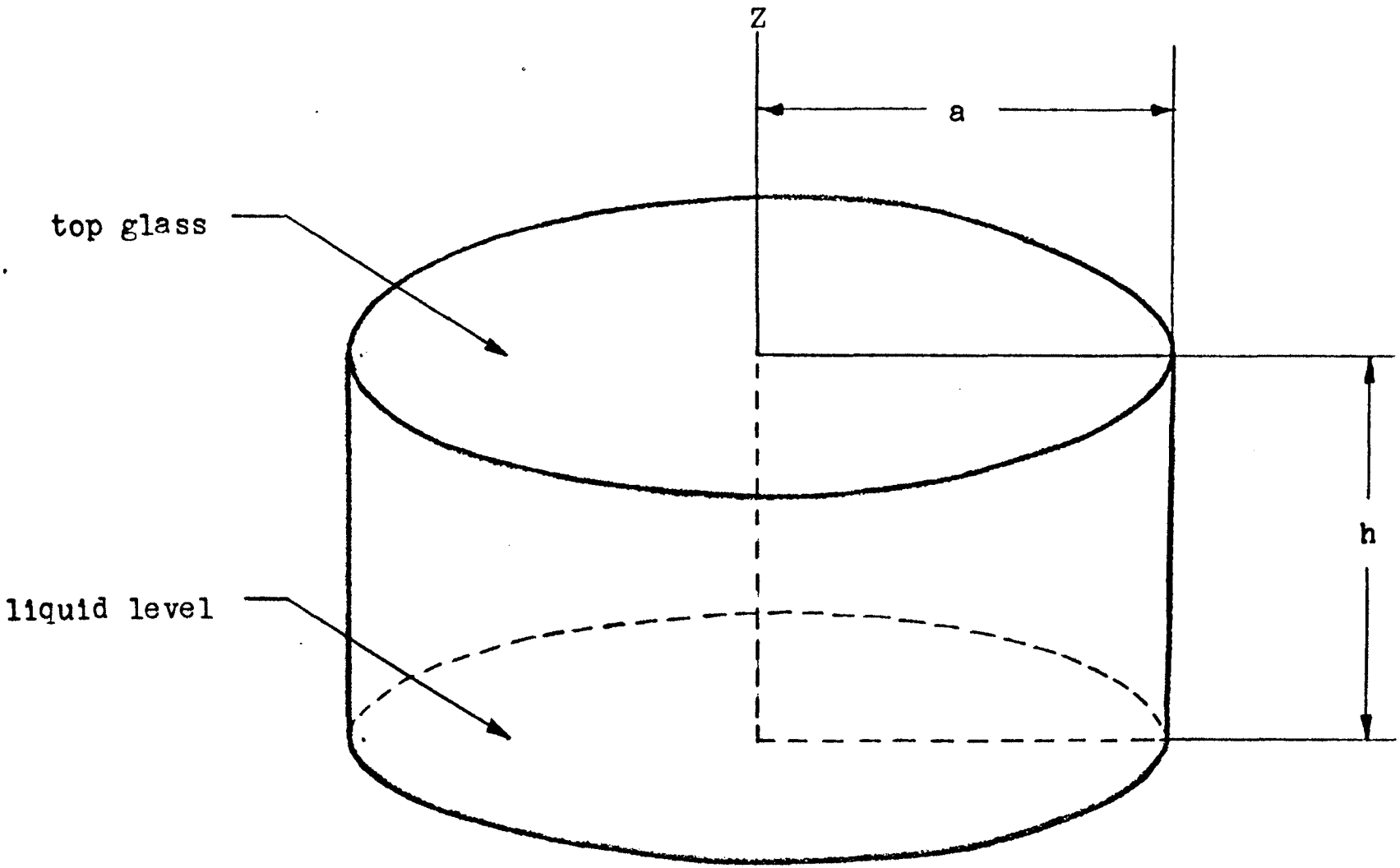

CYLINDRICAL COORDINATES FOR SECOND CALCULATION

Fig. 11

$$\frac{\partial^2 u}{\partial r^2} + \frac{1}{r}\frac{\partial u}{\partial r} + \frac{\partial^2 u}{\partial z^2} = 0 \qquad \begin{aligned} u(r,0) &= 0 \quad 0 \le r \le a \\ u(r,h) &= T \\ u(a,z) &= \frac{Tz}{h} \quad 0 \le z \le h \end{aligned}$$

The solution is obtained after making the change of variable:

$$v(r,z) = u(r,z) - Tz/h.$$

Then the equivalent problem in terms of $v(r,z)$ is

$$\frac{\partial^2 v}{\partial r^2} + 1/r\,\frac{\partial v}{\partial r} + \frac{\partial^2 v}{\partial z^2} = 0 \qquad \begin{aligned} v(r,0) &= 0 \\ v(r,h) &= 0 \\ v(a,z) &= 0 \end{aligned} .$$

The solution is $v(r,z) = 0$. Hence $u(r,z) = Tz/h$ and the isotherms are equally spaced horizontal planes. This means that near the center the top-bottom gradient is constant.

The first measurement in this series is designed to determine the top-bottom gradient near the center of the cloud chamber. A 0.002 inch diameter chromel-alumel thermocouple, obtained from Omega Engineering, was used. The cold junction was placed on the chamber wall below the liquid level. The thermocouple was bent at a 90° angle and rotated from top to bottom in the sensitive volume near the center of the chamber. The signal from the thermocouple was amplified with a California Instruments Model 3101-P3P DC amplifier and displayed on the Minneapolis-Honeywell Visicorder using a type M-400 galvanometer. The results, shown in Fig. 12, indicate an almost constant temperature gradient near the center of the sensitive volume.

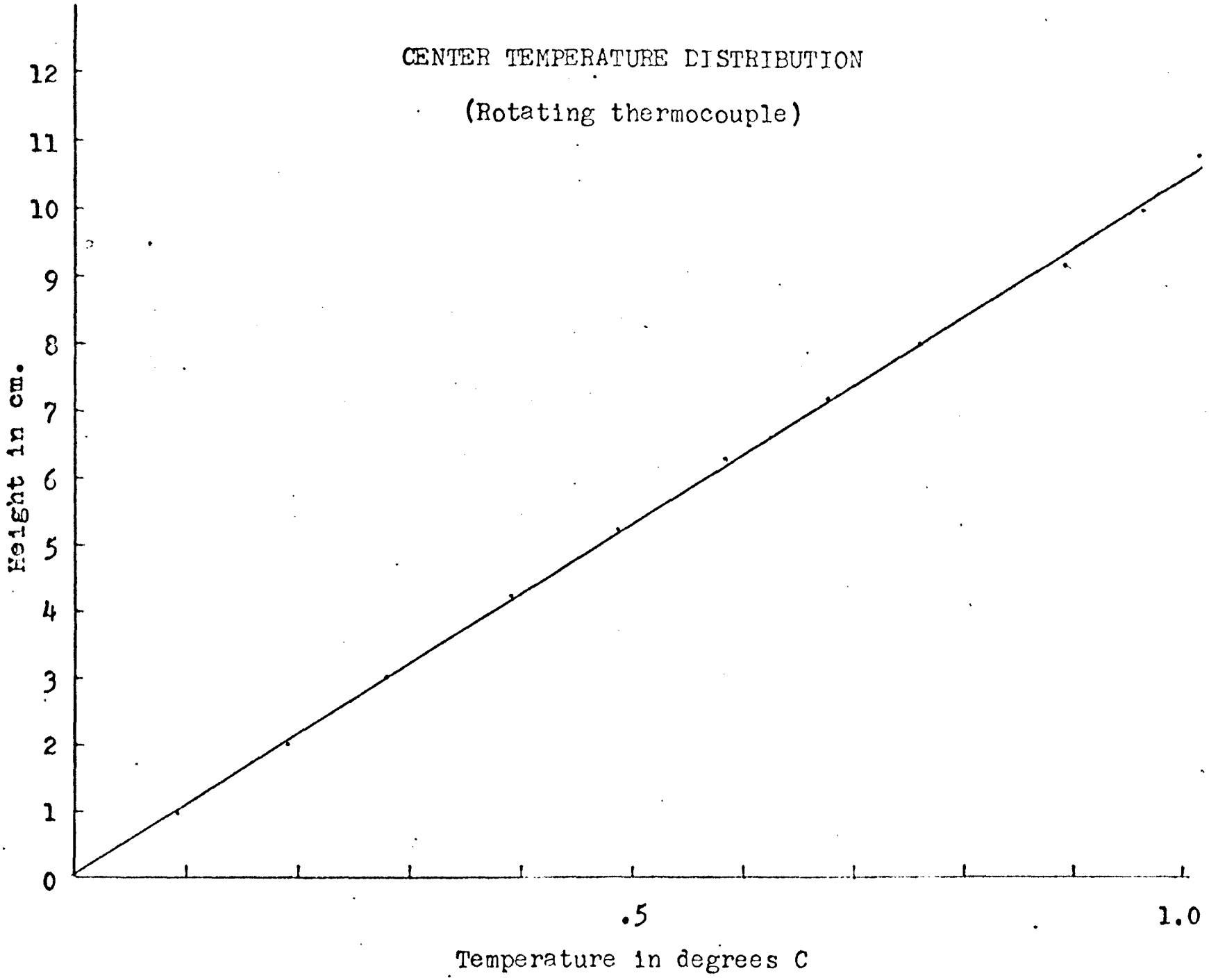
CENTER TEMPERATURE DISTRIBUTION
(Rotating thermocouple)
Height in cm.
12
11
10
9
8
7
6
5
4
3
2
1
0
.5
1.0
Temperature in degrees C

Fig. 12

This type of measurement was repeated with similar results each time. However, it was felt that the rotation of the thermocouple carried the junction too far from the center of the chamber to give reliable results. Also, it was difficult to measure the temperature near the walls using this particular thermocouple configuration. A new thermocouple was constructed to facilitate temperature measurements from the center to the side wall and from top to bottom. A 0.002 inch diameter chromel-alumel thermocouple was mounted in a stainless steel tube 0.25 inch in diameter and 11 inches in length. A teflon plug fitted with pieces of no.22 hypodermic needles serves as a hedder. The wires are threaded through the needles and sealed in with epoxy resin. The leads were made long enough so the hot junction could be moved up and down by merely bending the leads slightly. The 0.002 inch wires were sufficiently strong to support their own weight. The cold junction was enclosed in a heat sink and attached to the wall of the chamber below the liquid level by means of silicone grease and plastic electrical tape. The thermocouple could be pulled through the chamber from the side wall to the center by means of a slow-motion electric drive. The velocity of the moving thermocouple was approximately 0.01 cm/sec. However, measurements were always made with the thermocouple at rest.

The cloud chamber walls were insulated with tightly-fitting $\frac{1}{2}$ inch thick plastic foam. The top portion of the cloud chamber was also insulated with this foam. The insulation

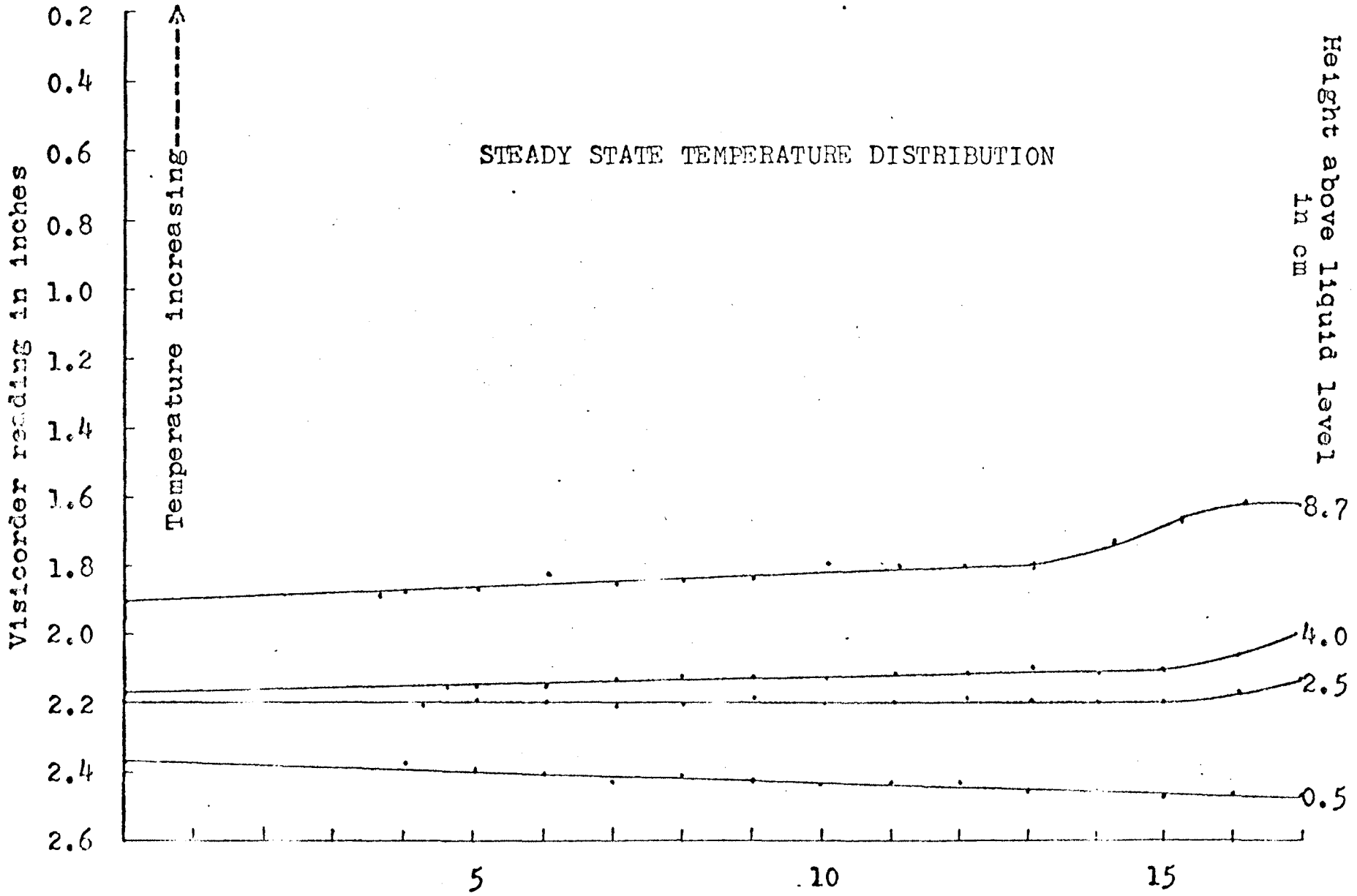
STEADY STATE TEMPERATURE DISTRIBUTION
Temperature increasing
Visicorder reading in inches
0.2
0.4
0.6
0.8
1.0
1.2
1.4
1.6
1.8
2.0
2.2
2.4
2.6
5
10
15
Radial distance in cm.
Height above liquid level in cm
8.7
4.0
2.5
0.5

Fig. 13

also served to maintain the temperature of the reference junction at a constant value.

The signal from the thermocouple was amplified by means of the California Instruments Corporation DC amplifier as before. Recordings were made on Visicorder paper. The position of the thermocouple junction was measured with a cathetometer (for determination of height above the liquid level) and with a jig (for measurement of distance from the center of the chamber).

Typical results of such measurements are shown in Fig. 13. Since the noise level of the Visicorder recordings was substantial, it was felt that the measurements might be meaningless. Also there was no way to check for possible amplifier drift. Since the signal was of the order of 30 microvolts, a drift of even 5 microvolts would be sufficient to invalidate the results. Therefore, the final series of measurements was made using a Hewlett-Packard Model 425A Microvoltmeter. The signal from the thermocouple was fed directly into the Microvoltmeter through a short length of shielded cable. The Microvoltmeter was zeroed on the 100 microvolt scale by shorting the input. Then the signal was read on that scale and the meter rezeroed. Measurements could then be made on lower voltage scales and zero drift monitored merely by shorting the input and noting the reading. Results of such measurements are shown in Fig. 14. For the region near the center of the chamber the isotherms are nearly horizontal planes. Both the Visicorder method

STEADY STATE TEMPERATURE DISTRIBUTION

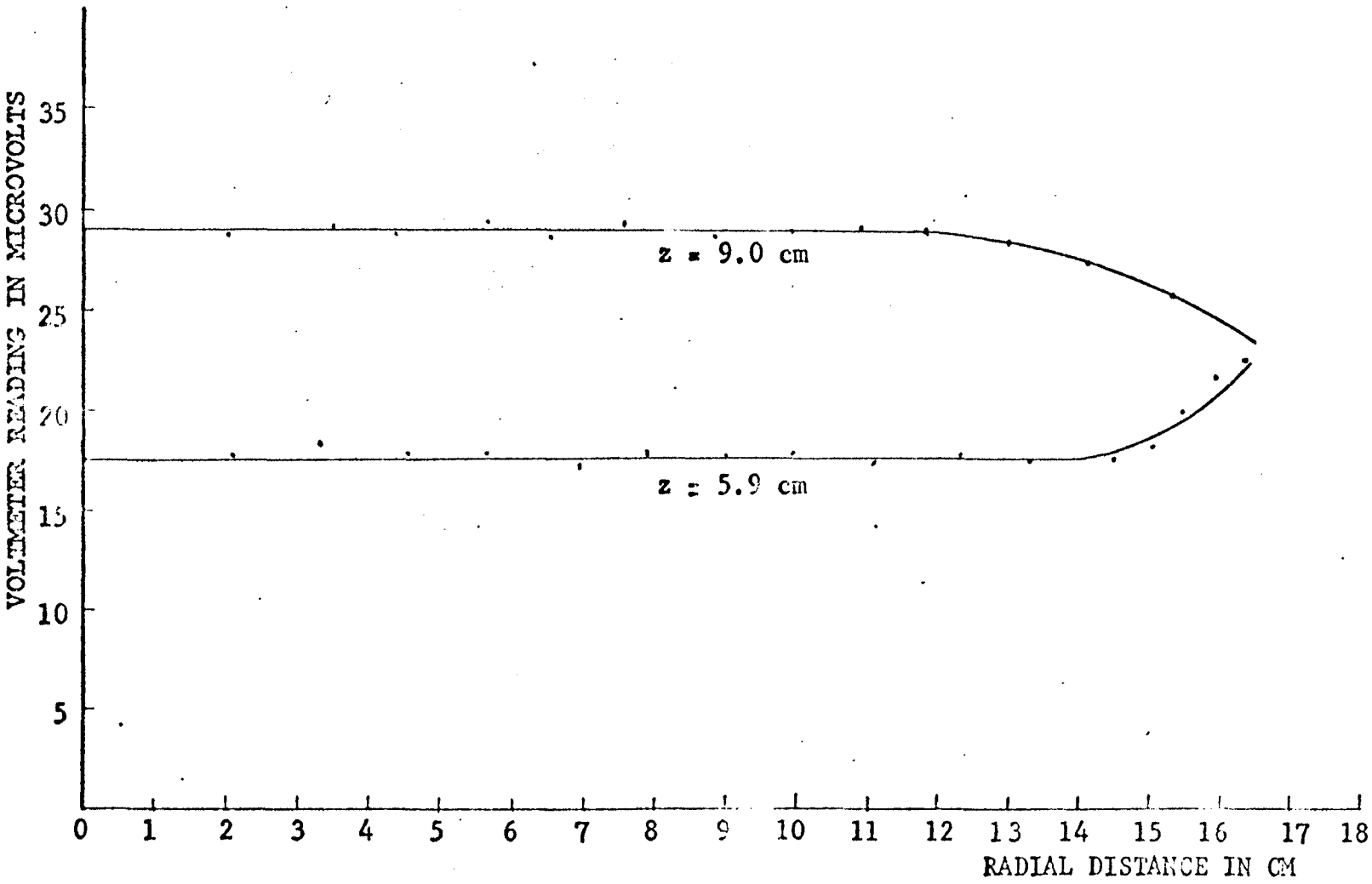

Fig. 14

and the Microvoltmeter method give similar results for the temperature distribution near the center of the sensitive volume. The isotherms in this region are horizontal planes more or less evenly spaced with respect to height above the liquid level. This tends to substantiate the results in Fig. 9, which indicate a linear top-bottom temperature distribution near the center.

The two methods of measurement do not, however, give the same results for the temperature distribution near the wall. The Visicorder results indicate a non-linear top-bottom temperature distribution near the wall. However, the Microvoltmeter results indicate that the temperature of the wall is a constant at least in the region midway between the top glass and the liquid level. The temperature of the wall is some constant intermediate to the temperatures of the liquid and the top glass. However, this question is of minor importance since only the central portion of the sensitive volume is useful for measurement purposes.

From this measurement it was decided that the initial temperature, T_1, at any point in the central portion of the chamber may be determined by monitoring the temperature of the top glass and the temperature of the liquid and using an equation as follows:

$$T_1 = \frac{T_T - T_B}{S_T - S_B} (S_o - S_B) + T_B$$

where: T_T = temperature at the top glass

T_B = temperature at the water surface

S_T = height of top glass

S_B = height of water surface

and S_o = height of plane where T_1 is desired.

A new thermocouple was designed to permit the water temperature to be measured more accurately. A small glass tube was sealed on one end and bent 90°. Oil was placed in the bottom of the tube to assure good thermal contact. The cold thermocouple junction was submerged in the oil and the glass tube passed through an O-ring sealed fitting in the wall of the chamber and submerged in the chamber liquid.

This new thermocouple will measure the temperature to 0.01 °C so that the initial temperature in the central portion of the chamber may be accurately determined.

2. THE EFFECT OF CONDENSATION OF THE TEMPERATURE MEASUREMENTS. It was mentioned in the introduction that it is impossible to measure the temperature in the cloud chamber during an expansion. Moisture is condensed on the sensing element long before a sufficient supersaturation is attained to nucleate water droplets. The latent heat evolved from this condensation gives an erroneous temperature reading. During the experiments to determine how long the various forms of the adiabatic laws remain valid, difficulties were encountered in measuring the temperature which were due to this effect.

Since it was recognized that it would be impossible to measure the temperature during an expansion, compressions were used so that the final temperature could be both measured and

calculated and the values compared. While the chamber was being programed for this compression cycle, it was noticed that the temperature trace was acting very strangely. The trace which resulted is shown is Fig. 15. It can be seen that the temperature measured by the thermocouple would not come up to its proper value immediately, but would attain some intermediate value and remain there for a short time before climbing on up to its proper value. The static temperature gradient at that point was excessively high (around $4^{\circ}C$ top to bottom), and it was felt that this may have had an adverse effect on the temperature measurement. Then the gradient was reduced to $1^{\circ}C$. The measurement was repeated for this top bottom gradient. It was found that the temperature measurement, instead of being improved, was worse. The trace remained at its intermediate level for an even longer time. This may be seen in Fig. 16.

It was finally decided that these strange results were due to water evaporating from the thermocouple element. Apparently, it took the water longer to evaporate when the gradient was turned down because the thermocouple collected more water at the lower static gradient prevailing in the cloud chamber.

To see whether or not it was really water on the thermocouple which was causing the disturbance, the chamber was allowed to sit in its quiescent state for about half an hour. After this time the chamber was activated and run through its compression cycle and a recording of P, V, and T was made of

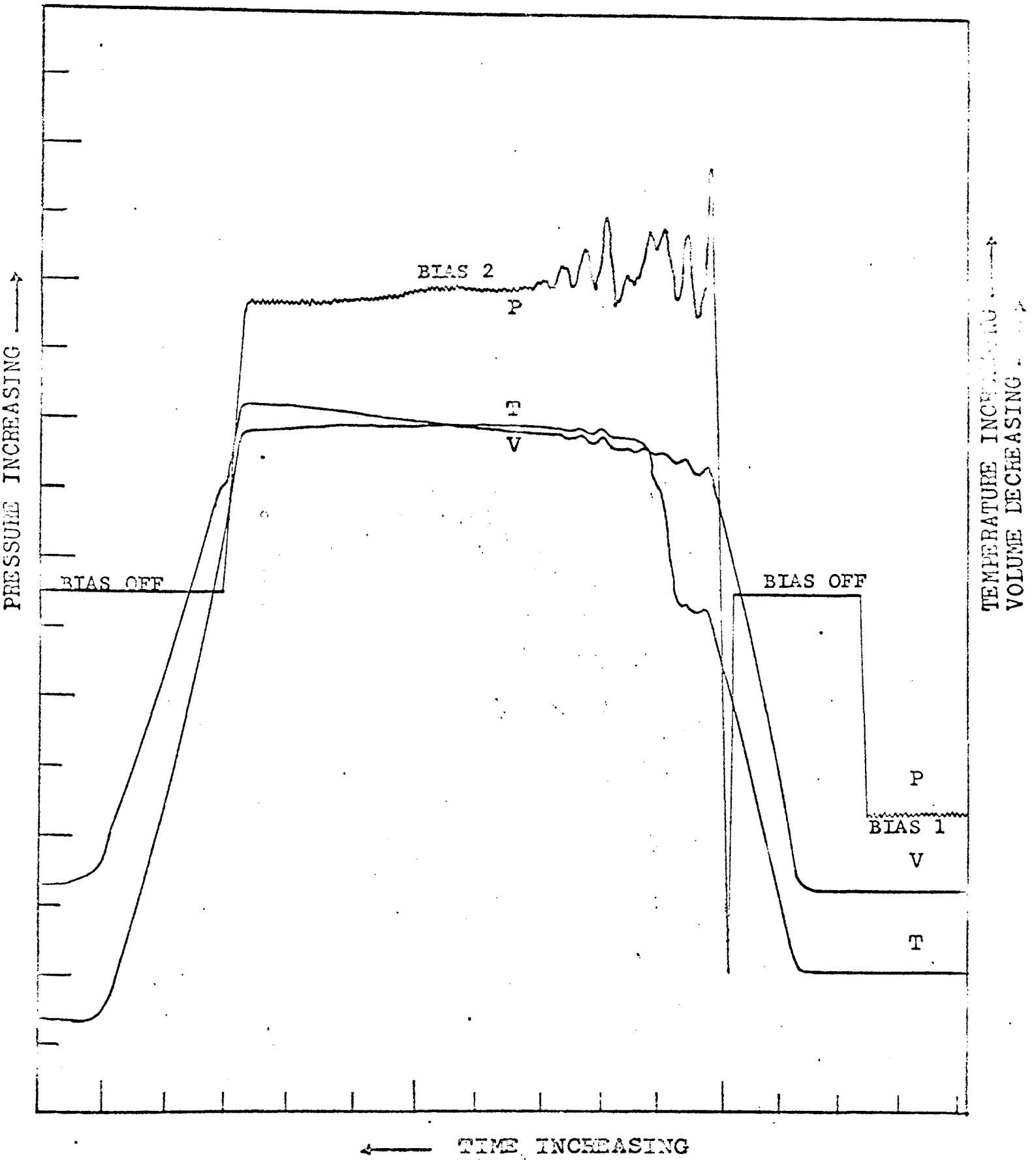
PRESSURE INCREASING
TEMPERATURE INCREASING
VOLUME DECREASING
BIAS 2
P
T
V
BIAS OFF
BIAS OFF
P
BIAS 1
V
T
TIME INCREASING

Fig. 15

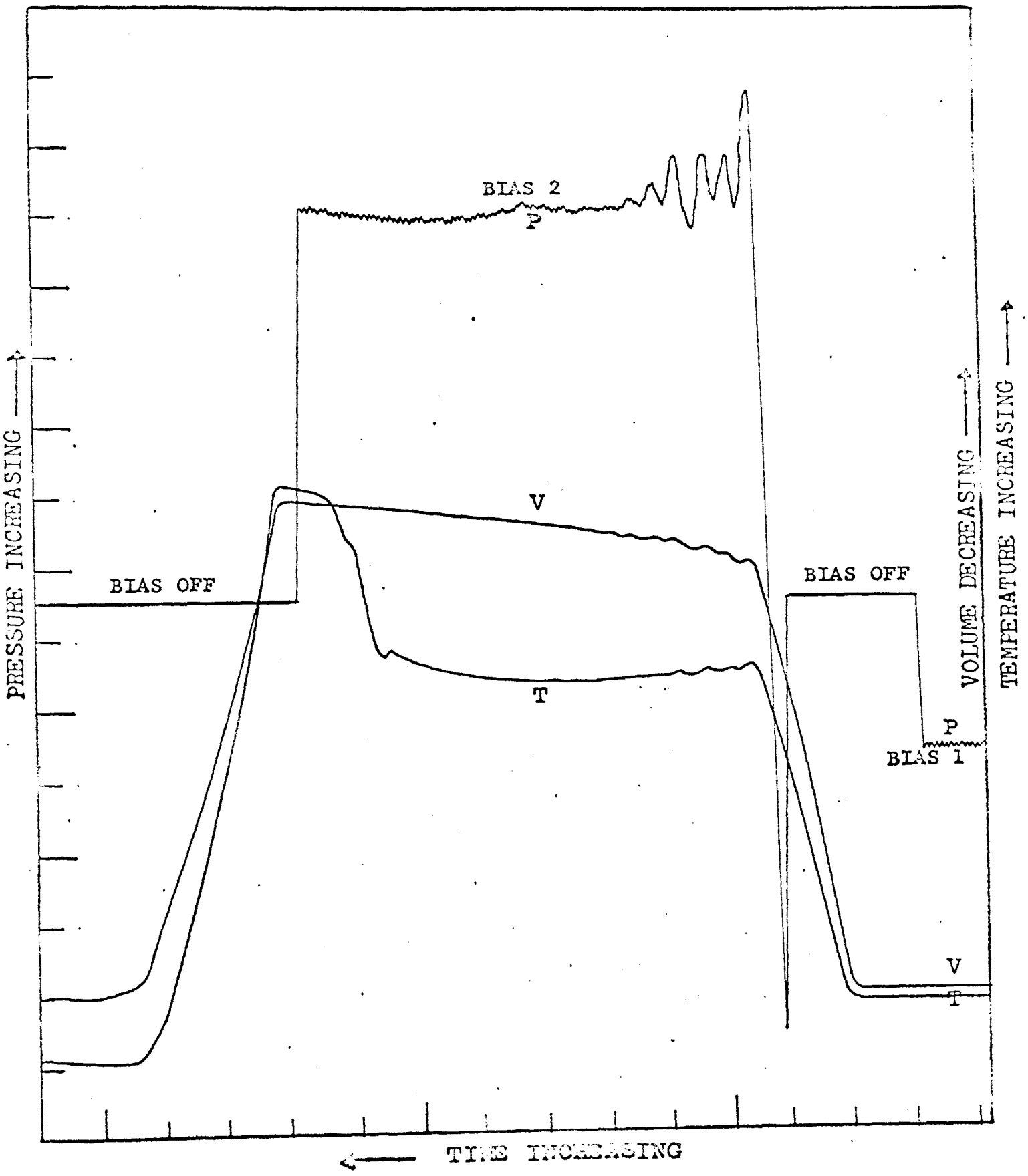
BIAS 2
P
V
BIAS OFF
BIAS OFF
T
P
BIAS 1
V
T
PRESSURE INCREASING
VOLUME DECREASING
TEMPERATURE INCREASING
TIME INCREASING

Fig. 16

this cycle. As can be seen in Fig. 17, the temperature trace came up to its proper value immediately. The next cycle however provided a temperature trace which was the same as Fig. 16.

It was concluded from this that the thermocouple was picking up moisture during the expansion back to the initial pressure. Apparently, even during the short 0.7 second interval that the chamber was in its compressed state, the gas had acquired a sizeable amount of vapor. During the expansion then, the chamber became supersaturated and some of the excess moisture condensed on the thermocouple. This hypothesis was further substantiated by the fact that the thermocouple and its fragile supports began to droop during the expansion due to the weight of the water collected on it.

It was decided to try expanding the chamber slower so that possibly the gas would not become supersaturated as highly. When this was tried, the trace of Fig. 18 resulted. In this trace, it is seen that the temperature comes to a steady final value, but during the re-expansion, it suddenly makes about a four degree rise, when it should be dropping. This effect could be due to one of two things. The first possible explanation is that the thermocouple is reading the correct final temperature, and during the expansion the chamber becomes saturated so that water is condensed on the thermocouple, liberating heat and causing a temperature rise. Since this was the result expected it

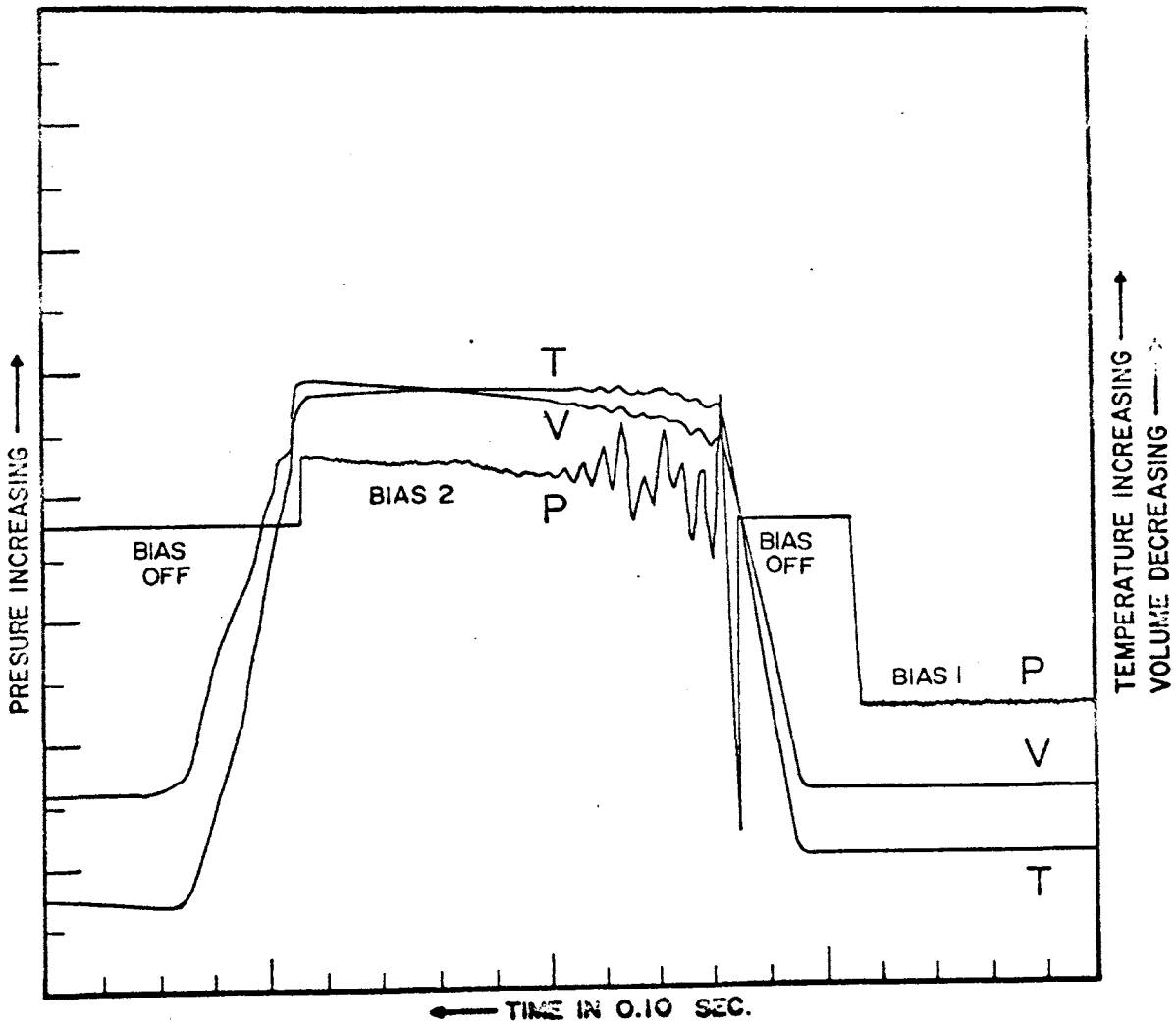
PRESURE INCREASING
TEMPERATURE INCREASING
VOLUME DECREASING
T
V
P
BIAS 2
BIAS OFF
BIAS OFF
BIAS 1
P
V
T
TIME IN 0.10 SEC.

Fig. 17

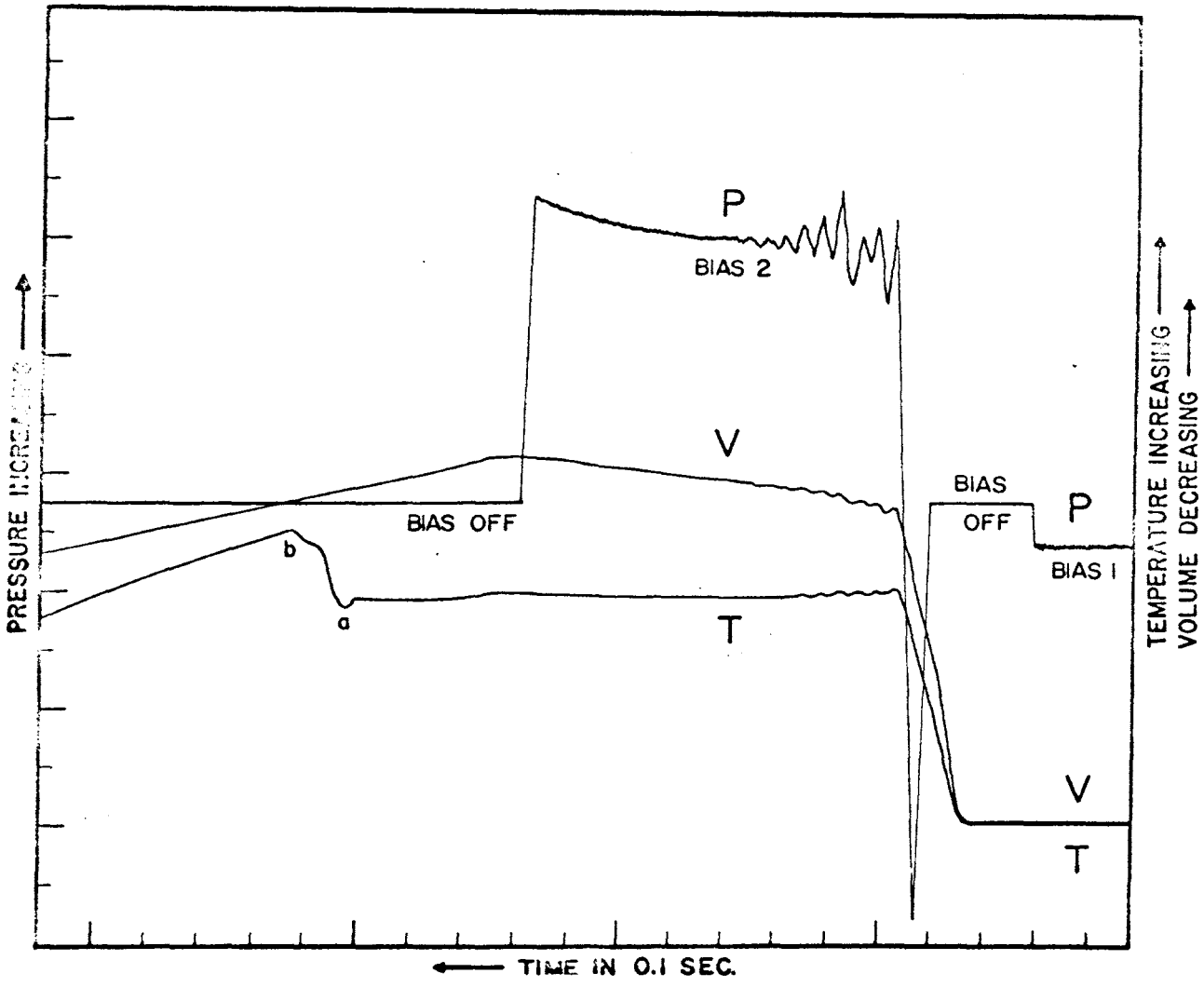
P
BIAS 2
V
BIAS OFF
b
a
T
BIAS
OFF
P
BIAS 1
V
T
TEMPERATURE INCREASING
VOLUME DECREASING
TIME IN 0.1 SEC.

Fig. 18

was at first thought that this was the case. However, a more careful examination of the results revealed that the second alternative was the case. The thermocouple acquired even more moisture during the slow expansion of the previous cycle. The temperature indicated by the thermocouple was lower than the temperature calculated from $T_1 P^{\frac{1-\gamma}{\gamma}} = T_2$, due to the evaporation of water from the thermocouple so that the temperature then rose to its proper value at point "b" on the temperature curve. The sudden dip in the temperature curve at point "a" has not been properly explained. One possible explanation is that the last trace of water evaporates more rapidly than the rest of the water. This feature is characteristic of all the recordings and can also be noticed in Fig. 16.

Still another method was then tried to get rid of the annoying effect of water on the thermocouple so that the test of the adiabatic laws could proceed. The Peltier effect was utilized by passing a current through the thermocouple in the proper direction to heat the junction. It was found that this plus the added effect of Joule heating effectively removed the water which had collected on the thermocouple. The thermocouple then read the proper final temperature. When the data to determine how long the adiabatic laws remain valid was run, the chamber was allowed to remain in the quiescent state for a half hour, and then about two minutes before the compression was made, the thermocouple was heated. Thus every attempt was made to assure that the thermocouple

was dry during the measurements.

The above difficulties in obtaining an accurate temperature measurement even during a compression serve to vividly illustrate the futility of attempting to measure temperature during an expansion while the chamber is supersaturated. All such attempts are doomed to failure so that it can be seen that it is necessary to use one of the forms of the adiabatic law to determine the final temperature. Since the problem of water on the thermocouple was finally overcome, it was then possible to check the validity of this procedure.

3. A TEST OF HEAT FLOW INTO THE CHAMBER. In order to test the validity of using the adiabatic laws to determine the final temperature, the chamber was programed with a cycle consisting of a fast compression from 530 inches of water, a continuing compression holding the pressure reasonably steady for over 0.7 seconds, and an expansion back to 530 inches of water. It was found that it was necessary to utilize three continuing compression valves with different orifice sizes, operating in a rather complex overlaping sequence, in order to hold the pressure steady for 0.7 seconds. This is because the boundary layer expansion effect is very severe immediately after the fast compression, but this expansion diminishes rapidly as the thermal gradient near the walls of the chamber decreases so that less and less correction is needed as time progresses.

The actual form of this expansion due to boundary layer

cooling versus time is approximately that of a decaying exponential. An actual trace showing this effect is given in Fig. 19. This is a trace of the pressure, volume, and temperature when the continuing compression was not employed. It will be noticed that the pressure drops precipitously immediately after the compression. This is because there is a temperature rise of about 25°C right after the compression, which is confined to a very narrow region of gas next to the walls so that the gradient is very large. This flow of heat decreases rapidly as the gradient decreases.

The use of the continuing compression yields pressure, temperature, and volume traces such as Fig. 20. It is now seen that it is possible to hold the pressure steady for almost a second, except for an unavoidable oscillation possibly due to the undamped vibration of the piston. The temperature also remains constant during this interval except at the very end when the effects of heat conduction are finally beginning to effect the temperature. The adiabatic law $T P^{\frac{1-\gamma}{\gamma}} = K_1$ was used to check exactly how long the center remains adiabatic when the continuing compression technique was used. A calculation was made every .05 seconds during the secondary compression. The results are given in Table II. Fig. 21 is a curve drawn from these results. It can be seen that the center remains adiabatic for 0.3 seconds which approximately supports Carstens[6] calculated time of 0.5 seconds.

The volume that is being measured is the entire volume

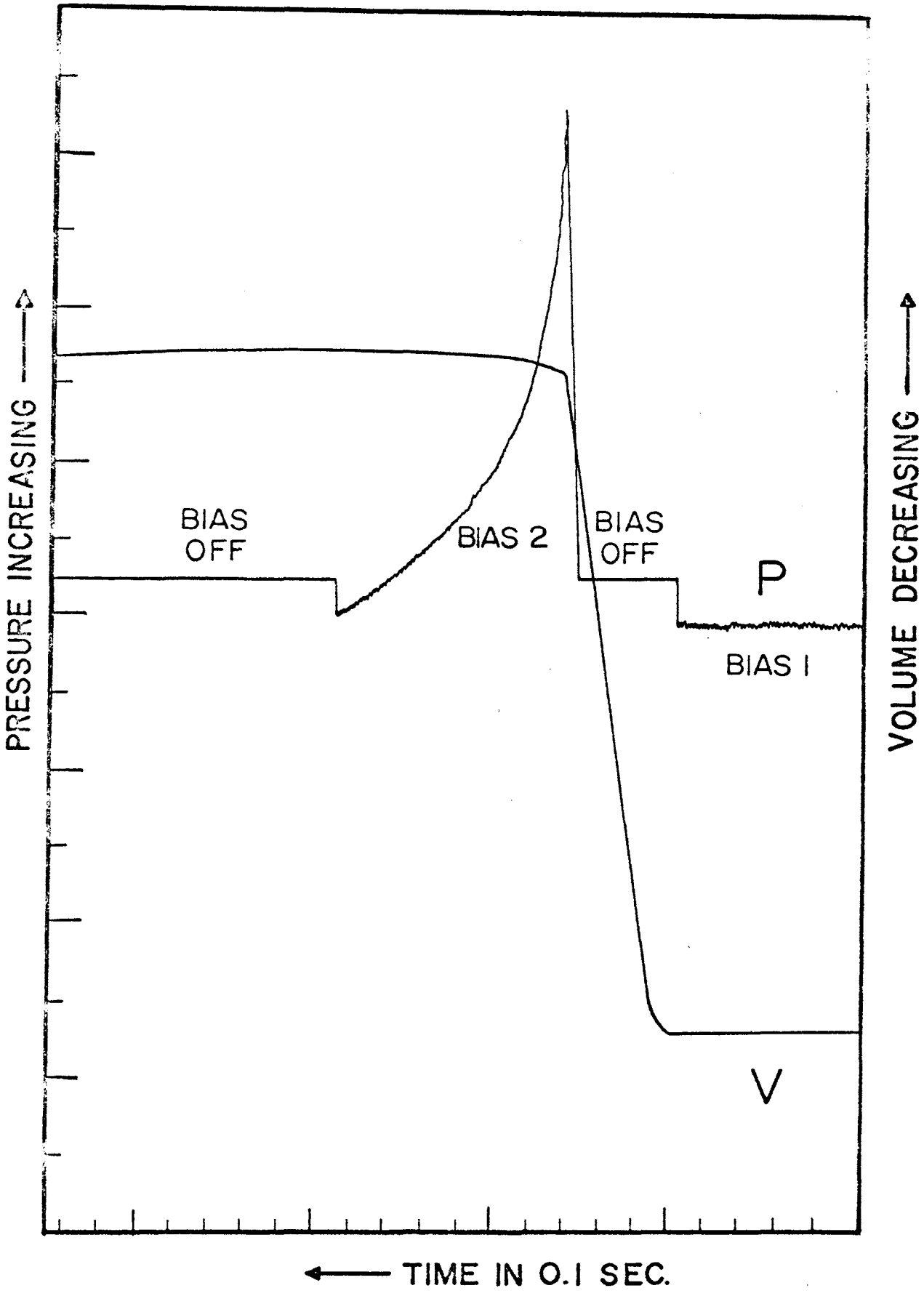
PRESSURE INCREASING
VOLUME DECREASING
BIAS OFF
BIAS 2
BIAS OFF
P
BIAS I
V
TIME IN 0.1 SEC.

Fig. 19

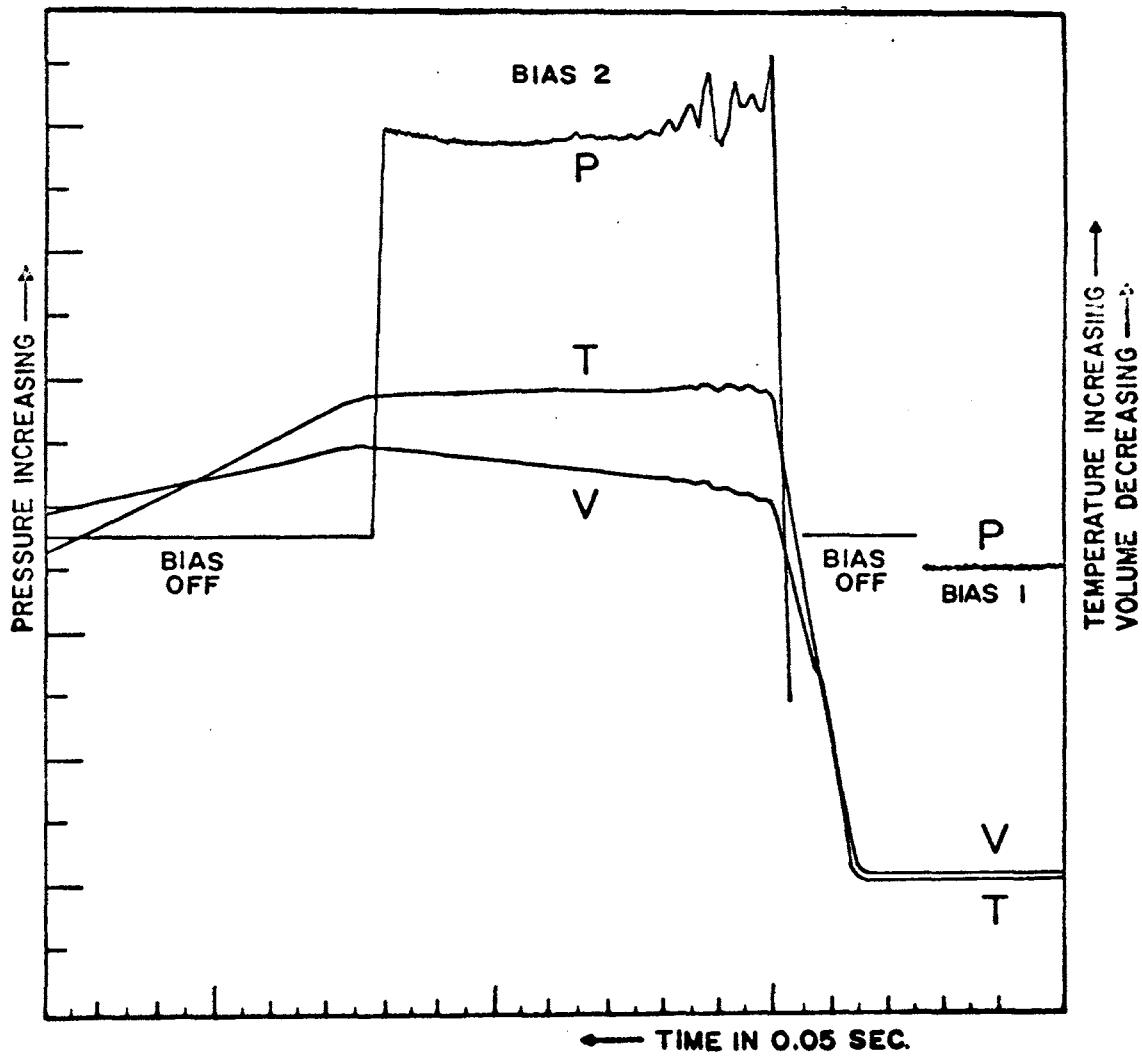
BIAS 2
P
T
V
BIAS
OFF
BIAS
OFF
P
BIAS 1
V
T
PRESSURE INCREASING
TEMPERATURE INCREASING
VOLUME DECREASING
TIME IN 0.05 SEC.

Fig.20

Table II

Time	P	T	$P^{\frac{1-\gamma}{\gamma}}$	$TP^{\frac{1-\gamma}{\gamma}}$
0 seconds	528.9 in. H_2O	293.66°K	.09252	27.17
0.10	645.4	316.62	.08578	27.16
0.15	645.8	316.73	.08576	27.16
0.20	646.5	316.97	.08572	27.17
0.25	646.0	316.79	.08575	27.16
0.30	645.2	316.71	.08579	27.17
0.35	646.4	316.88	.08572	27.16
0.40	647.7	316.97	.08566	27.15
0.45	647.2	316.79	.08569	27.15
0.50	647.3	316.71	.08568	27.14
0.55	647.5	316.53	.08567	27.12
0.60	647.6	316.44	.08567	27.11
0.65	647.6	316.36	.08567	27.10
0.70	647.6	316.18	.08567	27.08
0.75	647.7	315.93	.08566	27.06
0.80	647.8	315.75	.08566	27.05

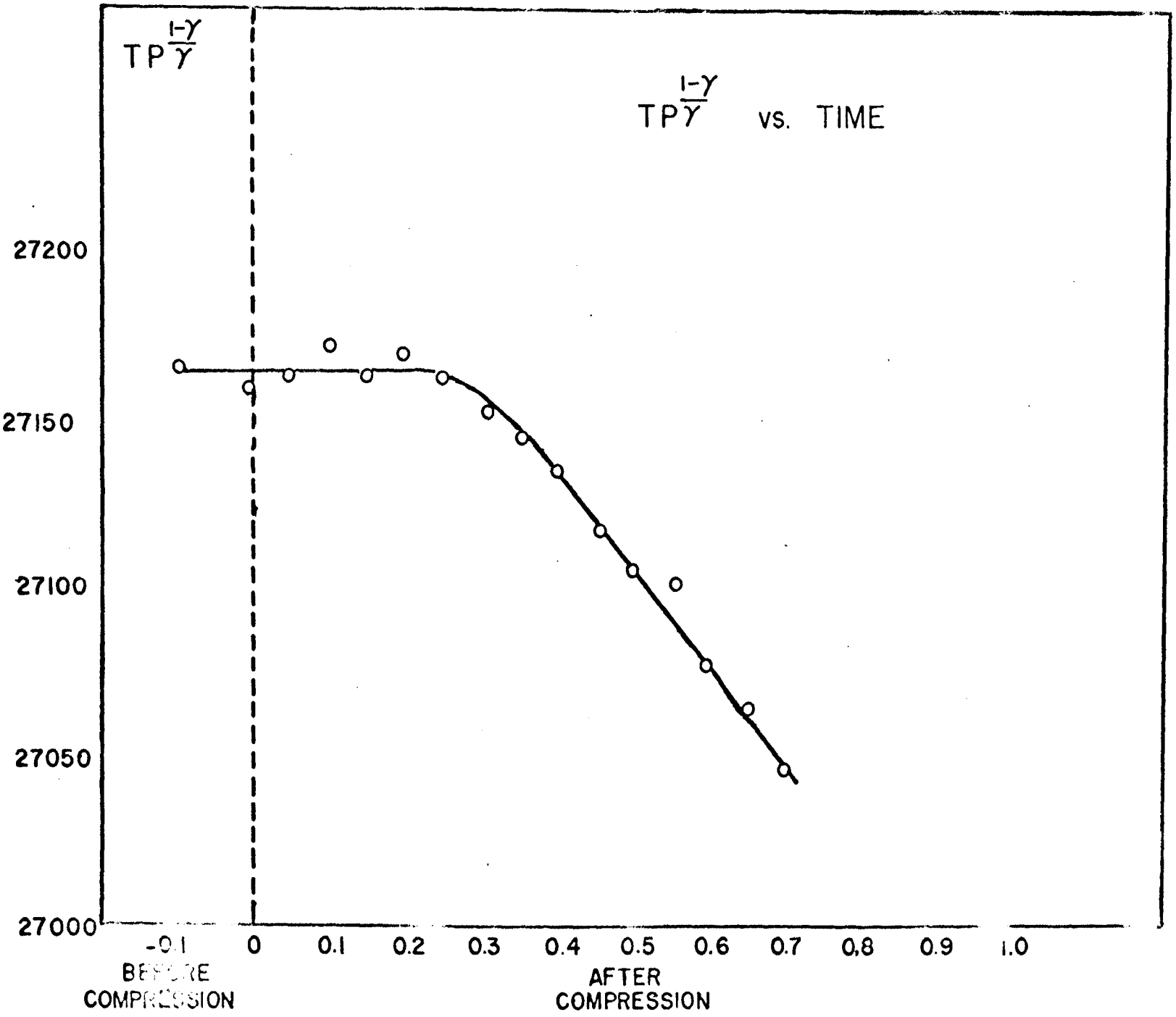
$TP^{\frac{1-\gamma}{\gamma}}$
$TP^{\frac{1-\gamma}{\gamma}}$ vs. TIME
27200
27150
27100
27050
27000
-0.1
0
0.1
0.2
0.3
0.4
0.5
0.6
0.7
0.8
0.9
1.0
BEFORE COMPRESSION
AFTER COMPRESSION
TIME in SECONDS

Fig. 21

of the gas-vapor mixture but the volume which remains adiabatic is decreasing during the continuing compression. There is no way to measure the small volume in the center, around the thermocouple junction, which remains adiabatic so there is no way to utilize an adiabatic law involving V. It can be expected that $P V^{\gamma} = K_2$ and $T V^{\gamma-1} = K_3$ will fail almost immediately, growing worse as time progresses. In order to see how badly the $P V^{\gamma}$ and $T V^{\gamma-1}$ fail to be constant, these quantities were also calculated for 0.05 second intervals during the continuing compression. The results of these calculations are shown in Tables III and IV. Fig. 22 and 23 are curves drawn of these three quantities versus time. It can be seen that $P V^{\gamma}$ and $T V^{\gamma-1}$ fails immediately as expected.

Perhaps the reason for the large difference in these quantities at rest and in the compressed position is that the rubber diaphragm stretches out of shape during the compression. The calibration of volume was of necessity done with the piston at rest, but the diaphragm may have a different configuration during an expansion or compression so that the volume calibration does not hold while the piston is moving.

It can still be seen from the curves how the adiabatic laws involving volume fail during the interval while the pressure and temperature are being held constant.

This experiment was repeated for seven different compressions. The I B M 1620 computer on campus was programed

Table III

Time	P ± 0.05	V ± 0.01	V^{γ} ± 0.06	$PV^{\gamma} \times 10^5$ ± 40.
0 seconds	528.9 in. H_2o	9.00 lt.	34.52	.1826
0.10	645.4	8.32	30.42	.1963
0.15	645.8	8.29	30.24	.1953
0.20	646.5	8.28	30.18	.1951
0.25	646.0	8.28	30.18	.1950
0.30	645.2	8.27	30.12	.1943
0.35	646.4	8.26	30.06	.1943
0.40	647.7	8.24	29.95	.1940
0.45	647.2	8.24	29.95	.1938
0.50	647.3	8.23	29.89	.1935
0.55	647.5	8.22	29.83	.1931
0.60	647.6	8.22	29.83	.1932
0.65	647.6	8.21	29.77	.1928
0.70	647.6	8.20	29.72	.1924
0.75	647.7	8.20	29.71	.1924
0.80	647.8	8.20	29.71	.1925

Table IV

Time	T ± 0.05	V ± 0.01	$V^{\gamma-1}$ ± 0.005	$TV^{\gamma-1}$ ± 2.0
0 seconds	293.66°K	9.00 lt.	3.863	1.134×10^3
0.10	316.62	8.32	3.656	1.158
0.15	316.73	8.29	3.648	1.155
0.20	316.97	8.28	3.645	1.155
0.25	316.79	8.28	3.645	1.155
0.30	316.71	8.27	3.642	1.153
0.35	316.88	8.26	3.639	1.153
0.40	316.97	8.24	3.634	1.152
0.45	316.79	8.24	3.634	1.151
0.50	316.71	8.23	3.632	1.150
0.55	316.53	8.22	3.629	1.149
0.60	316.24	8.22	3.629	1.148
0.65	316.36	8.21	3.626	1.147
0.70	316.18	8.20	3.634	1.146
0.75	315.93	8.20	3.624	1.145
0.80	315.75	8.20	3.624	1.144

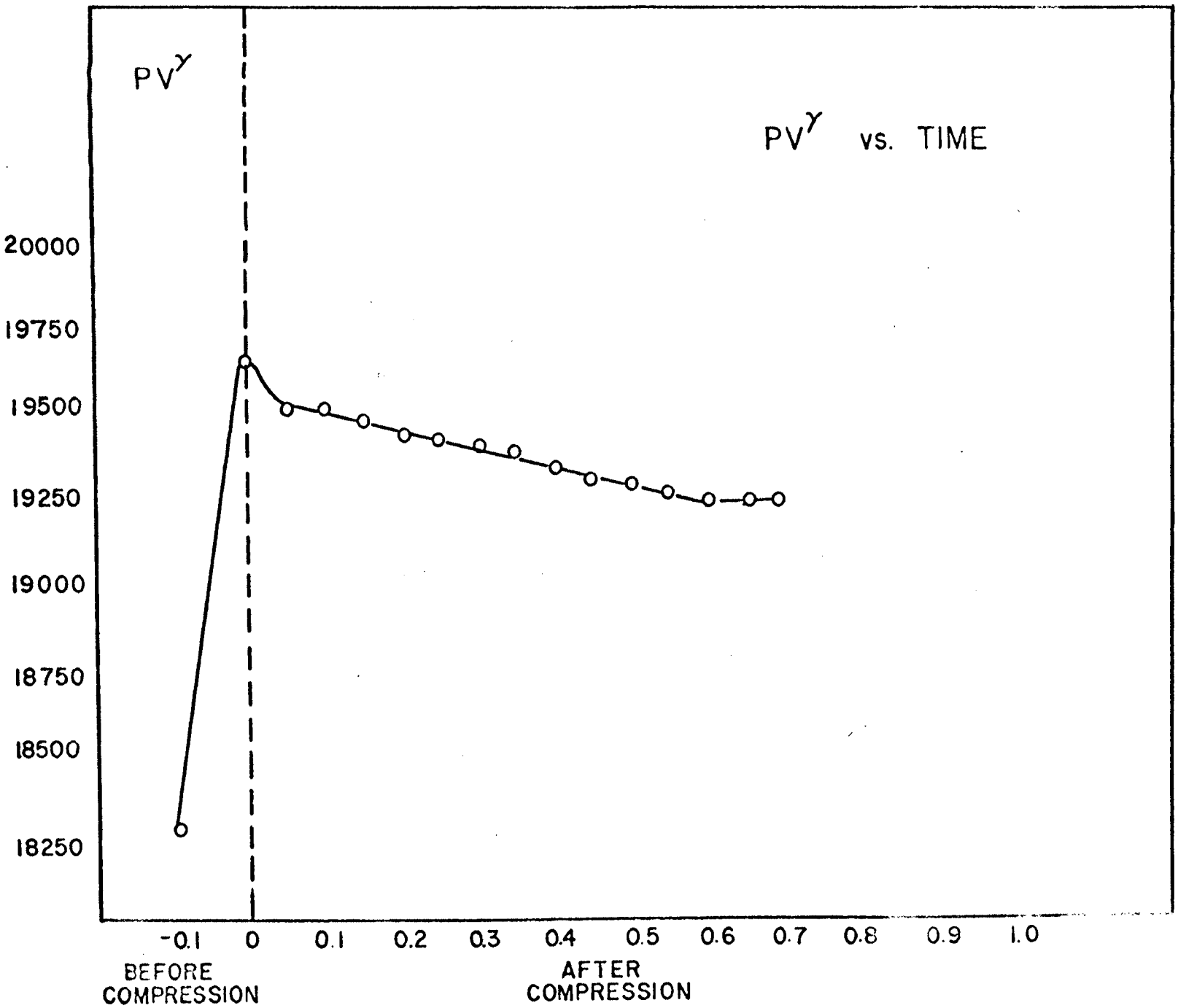
PV^γ
PV^γ vs. TIME
20000
19750
19500
19250
19000
18750
18500
18250
-0.1
0
0.1
0.2
0.3
0.4
0.5
0.6
0.7
0.8
0.9
1.0
BEFORE COMPRESSION
AFTER COMPRESSION
TIME in SECONDS

Fig. 22

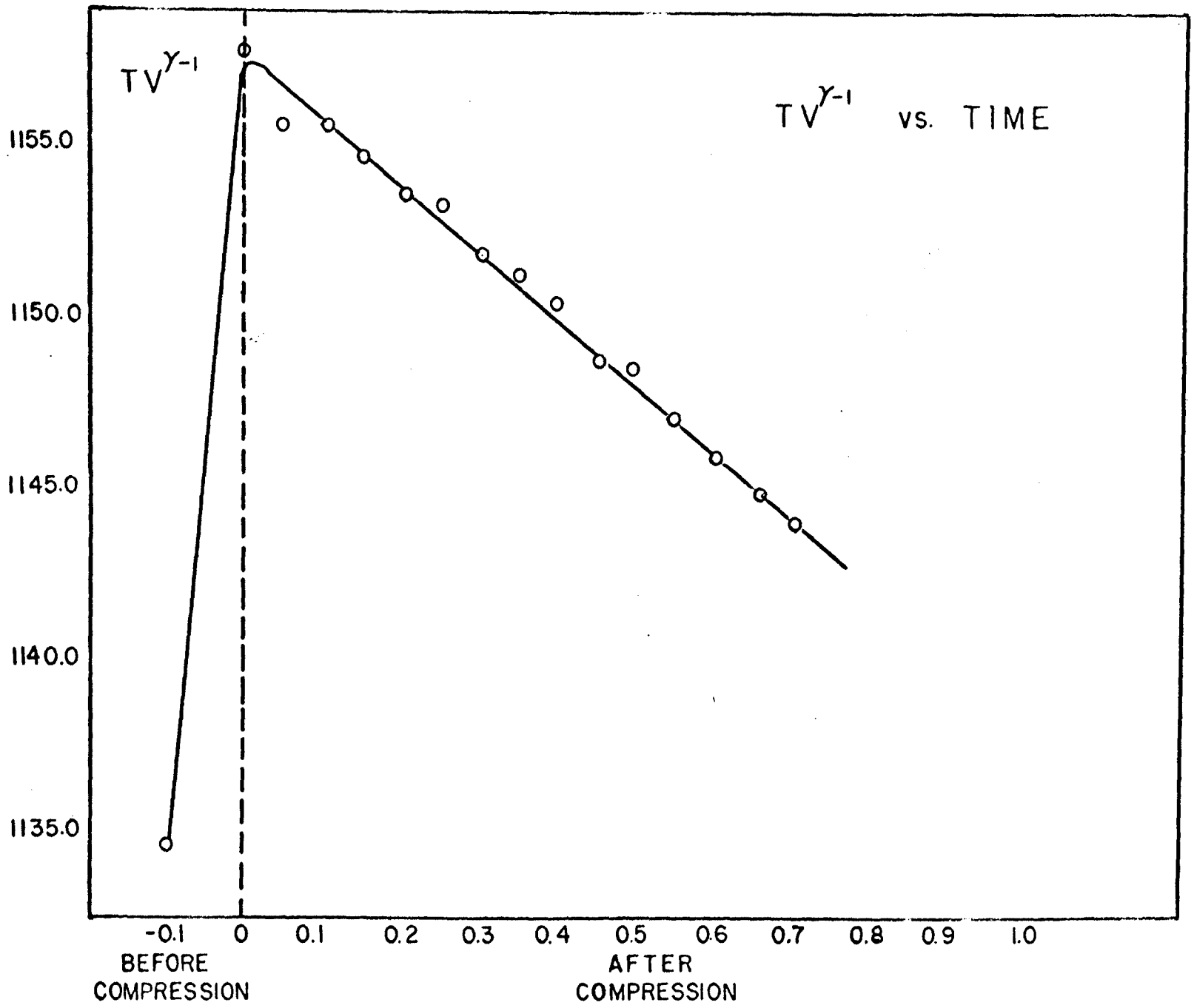
$TV^{\gamma-1}$
$TV^{\gamma-1}$ vs. TIME
1155.0
1150.0
1145.0
1140.0
1135.0
-0.1
0
0.1
0.2
0.3
0.4
0.5
0.6
0.7
0.8
0.9
1.0
BEFORE COMPRESSION
AFTER COMPRESSION
TIME in SECONDS

Fig. 23

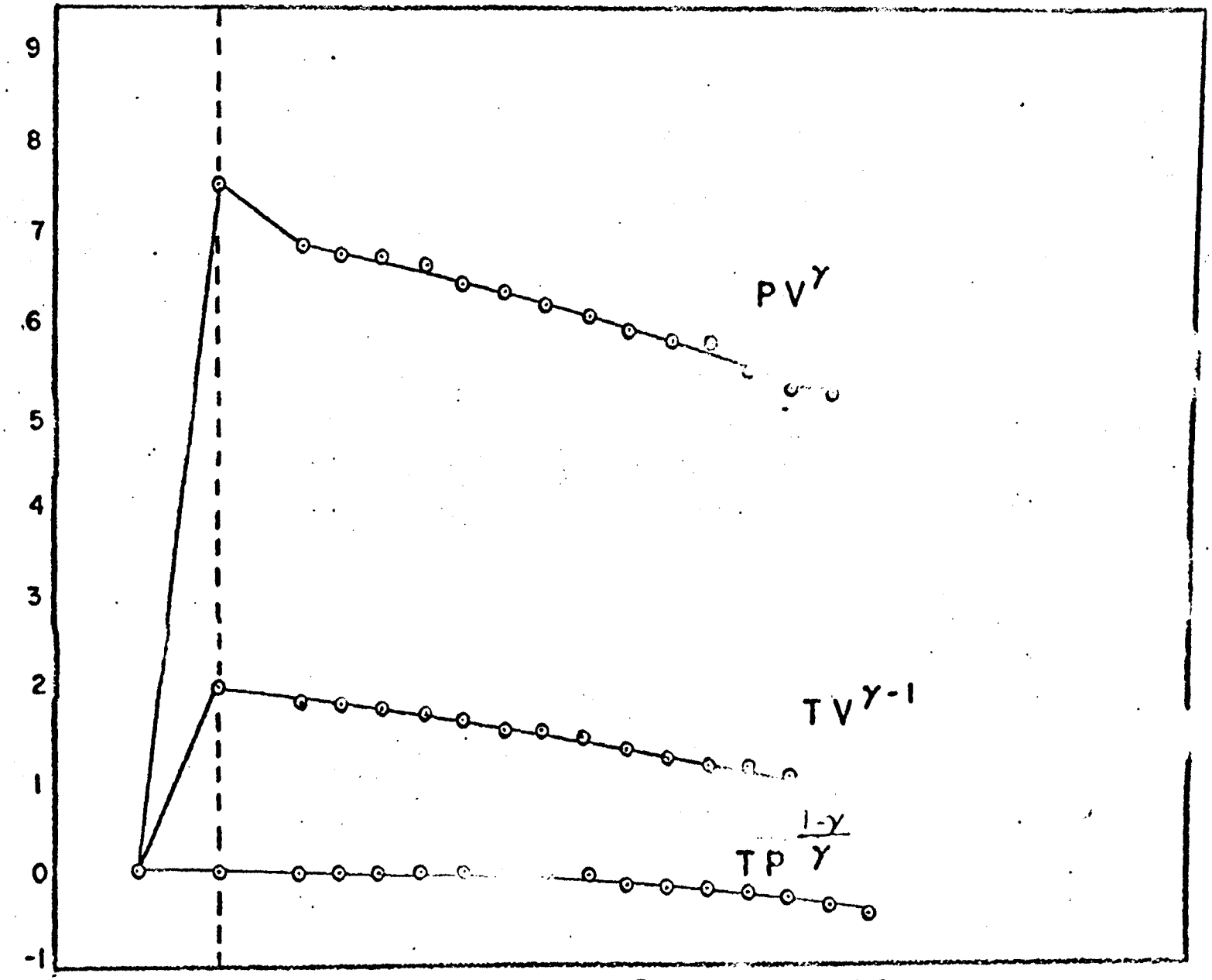
9
8
7
6
5
4
3
2
1
0
-1
PERCENT
DIVIATION
PV^{γ}
$TV^{\gamma-1}$
$Tp^{\frac{1-\gamma}{\gamma}}$
-0.1
0
0.1
0.2
0.3
0.4
0.5
0.6
0.7
0.8
BEFORE
COMPRESSION
AFTER COMPRESSION
TIME SECONDS

Fig. 24

to do the calculations. The results are displayed in appendix 1. The information dislayed in this section was taken from compression 1.

4. AN ATTEMPT TO MEASURE γ. The data obtained from the 7 compressions mentioned above was used to measure γ for the system. The results were also calculated on the I.B.M. 1620 computer. These results are also displayed in appendix 1.

The method was rather simple. The temperature measured by the thermocouple was taken as the true temperature. The temperature and pressure measurements were used in Eq. (14) to calculate the value for γ. The results from compression 1 was that $\gamma = 1.616$.

This value is quite a bit lower than γ calculated from Richarz's formula using Schmitt's and Dawbarn's values of γ for water vapor and helium. The value obtained from this calculation was 1.661 for the initial pressure and temperature in the chamber before compression 1 was performed.

The results of this experiment are rather inconclusive because γ varied from 1.616 to 1.590 over the 7 compressions. It is possible that a residual trace of water remained on the thermocouple during these compressions, thus causing the final temperature to be too low. The final temperature was calculated for each compression using γ computed from Schmitt's and Dawbarn's values for γ of water vapor and helium. The calculated temperature was 0.58 °C higher than the temperature measured by the thermocouple for the first

compression.

Since γ is the quantity which ultimately leads to the most error in the supersaturation, more work needs to be done to obtain this quantity as accurately as possible. The γ of helium makes the largest contribution to γ of the helium-vapor mixture. γ of water vapor only effects the total γ in the third decimal place.

Therefore, the chamber should be purged of water and the experiment repeated with pure dry helium in order to obtain the best γ for helium. Expansion of the same type used to obtain nucleation could be performed in the desiccated chamber instead of compressions since there would be no longer a problem of condensation on the thermocouple. In this way γ for helium in the proper temperature and pressure range could be found.

5. THE RECOVERY TIME OF THE CHAMBER. A cycle of the form described above was used to determine how long the chamber takes to return to its original temperature after an expansion. Again, a compression was used instead of an expansion to avoid condensation on the thermocouple. This type of cycle, where the chamber is expanded or compressed, held at the final pressure for an extended period of time, and then brought back to its initial pressure, will cause more heat pumping than the type of cycle normal used in experiments to investigate nucleation rates. The type of cycle used in nucleation experiments is shown in Fig.(25). Referring to this figure, the cycle from A to C is set up to form droplets,

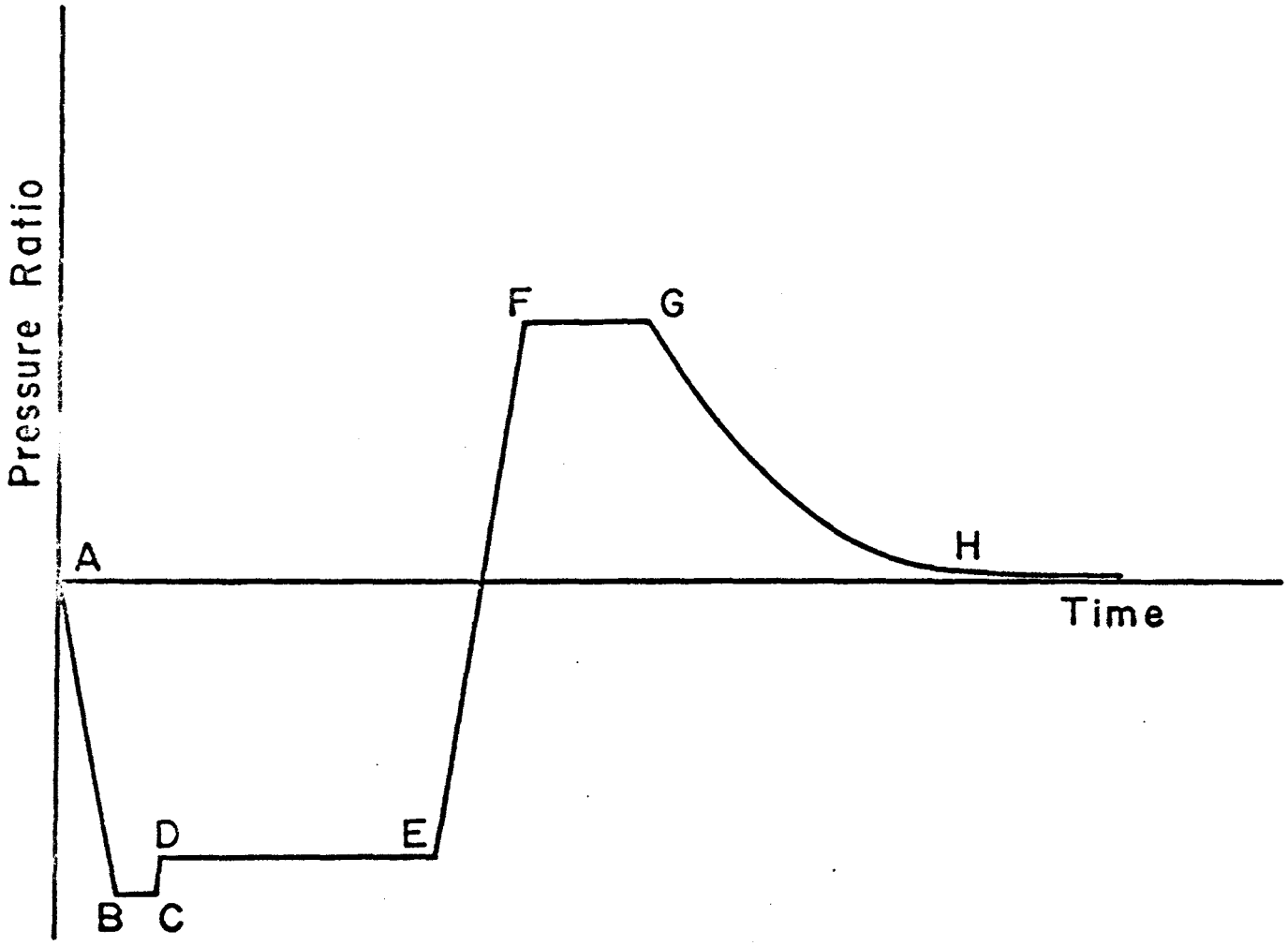

Fig. 25

A small compression cuts off the formation of new droplets from C to D, but allows the droplets which have been formed to grow to visible size from D to E. The cycle is then compressed to a pressure greater than the initial pressure from D to F. This evaporated the droplets. The chamber is held in this compressed state for a short time from Fto G. This allows the heat which flowed into the chamber during the expansion to flow out again. The chamber is them slowly expanded again from G to H. This slightly supersaturates the chamber which allows any residual re-evaporation nuclei to grow and fall into the liquid thus clearing the chamber of nuclei. The supersaturation is not high enough to form new droplets homogeneously.

Thus, it is seen that a great deal of the heat which flows in during the expansion will flow out again during the compression. This means the chamber will not take so long to return to equilibrium after the cycle is completed. This is why the cycle was chosen as it was for this experiment. It was desired to measure the longest time required for the chamber to return to its initial temperature.

It was felt that this experiment would simultaneously determine how long is required for the temperature gradient to return to its initial state. The junction of the thermocouple was not placed at the center of the chamber but about an inch and a half from the top. The temperature at the junction could not return to its initial value at that point until the temperature gradient had been properly reestablished.

The experimental procedure was very simple. The chamber was run through a cycle identical with that used to check the heat flow into the chamber. This time however, the Visicorder was not shut off after the compression was completed, but was allowed to run for the full duration of the cycle.

Just as expected, the temperature did not return to its initial value when the chamber was expanded back to its initial volume. Immediately after expansion the temperature was 2.62 ^{o}C too low due to the heat which had escaped the chamber. About three tenths seconds later the temperature rose 0.7 ^{o}C and two seconds after that the temperature fell to 3.14 ^{o}C below the initial temperature. These eratic effects are due to the turbulance which is caused by the convection currents.

Soon the turbulance ceased and 28 seconds later the temperature came back to its initial value. It can therefore be said that the three minute cycle which is used in nucleation experiments certainly allows time for the bulk temperature and temperature gradient to return to their initial values.

The three minute cycle is used to assure that sufficient time is allowed for the chamber to re-establish a state of saturation. Dawbarn[19] states that no difference is detectable in the results obtained from running the chamber on a two minute cycle and running it on a three minute cycle. Thus, surely the chamber has been properly saturated after a waiting interval of three minutes.

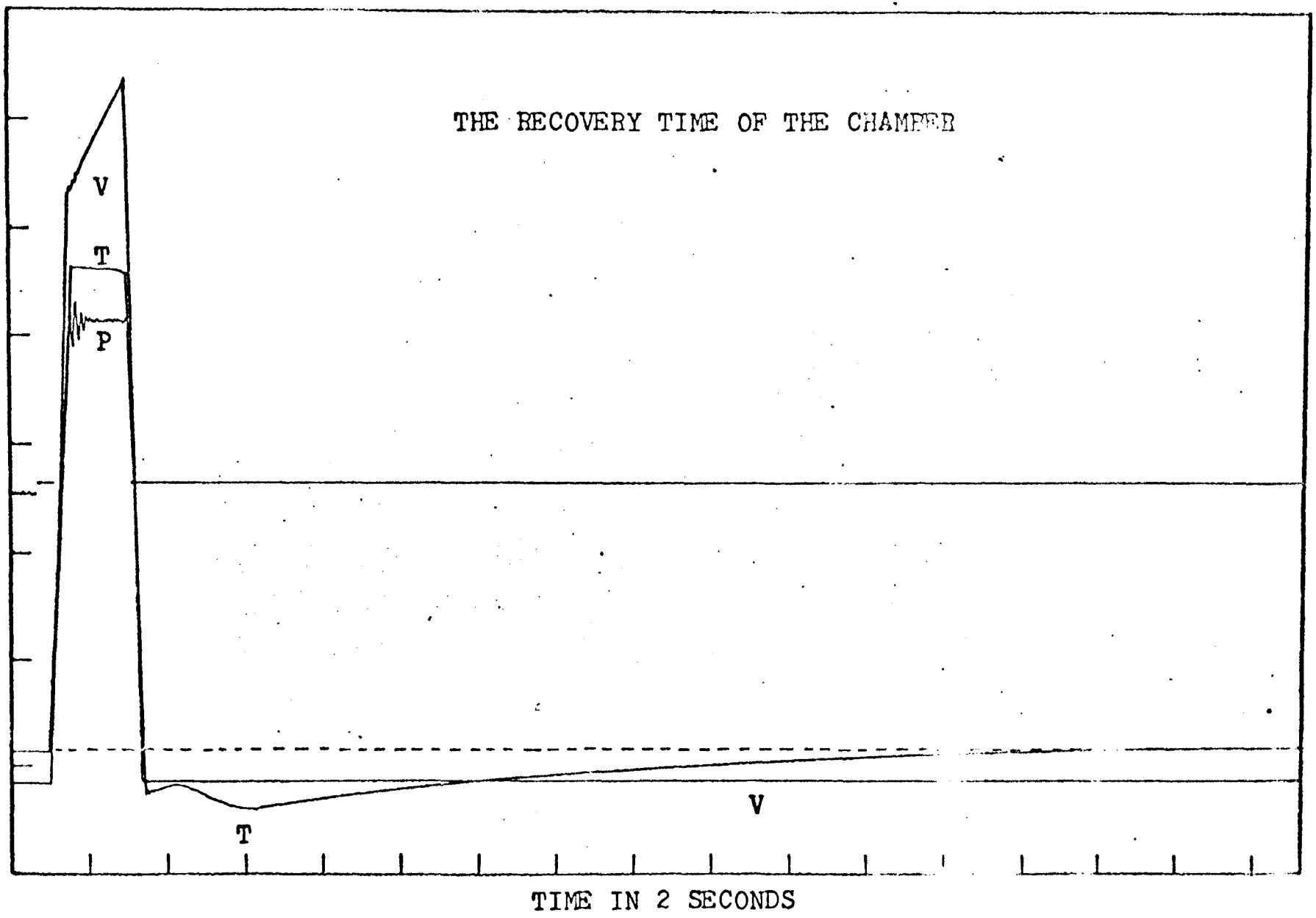

Fig. 26

6. SUMMARY. It has been found from an error analysis that ultimately the main source of error in measuring nucleation rates is a limited knowledge of γ of the carrier gas, helium. An uncertainty in the initial temperature also contributes a much smaller but still significant error. The pressures are presently being measured with sufficient precision that they cause negligible error.

An effort was made to measure γ more accurately, but the results were inconclusive. The method used does show promise for future work, however, if the water is removed from the chamber during the measurement.. Since insufficient knowledge of γ for helium is the largest obstacle to an accurate measurement of nucleation rates, Dawbarn's determination of γ should be checked experimentally.

The isotherms of the cloud chamber at rest were measured. The temperature of the top glass and the liquid are now monitored by thermocouples. From a knowledge of the top to bottom temperature difference and the form of the isotherms, it is now possible to determine the temperature near the center with fair precision. This is a great improvement over the method of attaching a thermometer to the side of the chamber at the water level with wax, which was used by Allard.

An experimental check was made of Carsten's approximate calculation of heat flow into the chamber. It was found that it takes 0.3 seconds for heat to reach the center so that the adiabatic law involving P and T may be used to calculate the final temperature. The value 0.3 seconds is in better agree-

ment with Carsten's value of 0.5 seconds than it appears. His calculations are for an expansion from 20 °C to 0 °C. The measurement is for a compression from 20 °C to 43 °C. A smaller amount of time should be expected for the measurement at this higher temperature due to parameters such as diffusion coefficients which are temperature dependent.

A measurement was made of how long is required for the chamber to re-establish equilibrium after a compression. It was found that the three minute waiting interval between expansions, presently being used, is surely sufficient time for the chamber to equilibrate.

A knowledge of the operating characteristics of the cloud chamber however, allows the chamber to be programmed to avoid, in as much as possible, errors due to indetermined operational characteristics.

APPENDIX I

DATE 9/16/64 EXPERIMENT NO. 5

CALIBRATION DATA

INCHES	INITIAL PRESSURE	INCHES	FINAL PRESSURE
3.50	140.0	2.03	248.5

COMPRESSION NO. 1

FINAL TEMP. CALCULATED = 317.29
FINAL TEMP. MEASURED = 316.71

COMPUTED VALUE OF GAMMA = 1.6156

TIME	PRESSURE	TEMPERATURE	CONSTANT	PERCENT DEV.
0.00	528.8	293.66	26.924	0.000
.10	644.3	316.62	26.924	-.001
.15	644.7	316.71	26.924	.000
.20	645.5	316.97	26.935	.040
.25	644.9	316.79	26.929	.018
.30	644.1	316.71	26.935	.040
.35	645.3	316.88	26.930	.019
.40	646.7	316.97	26.915	-.036
.45	646.2	316.79	26.909	-.058
.50	646.3	316.71	26.899	-.095
.55	646.6	316.53	26.880	-.163
.60	646.7	316.45	26.871	-.197
.65	646.7	316.36	26.864	-.225
.70	646.7	316.18	26.849	-.280
.75	646.8	315.92	26.825	-.369
.80	646.9	315.75	26.808	-.431

COMPRESSION NO. 2

FINAL TEMP. CALCULATED = 317.19
FINAL TEMP. MEASURED = 316.36

COMPUTED VALUE OF GAMMA = 1.6051

TIME	PRESSURE	TEMPERATURE	CONSTANT	PERCENT DEV.
0.00	529.5	293.66	27.603	0.000
.10	647.8	316.53	27.574	-.107
.15	644.8	316.36	27.608	.016
.20	645.1	316.36	27.603	.000
.25	645.0	316.36	27.604	.003
.30	644.5	316.27	27.606	.008
.35	643.9	316.10	27.599	-.014
.40	647.4	316.62	27.588	-.054
.45	646.0	316.36	27.589	-.052
.50	646.7	316.45	27.585	-.067
.55	646.7	316.10	27.554	-.177
.60	646.9	316.01	27.543	-.217
.65	646.8	315.83	27.530	-.266
.70	647.0	315.66	27.512	-.331
.75	647.1	315.57	27.503	-.365
.80	647.2	315.22	27.469	-.485

COMPRESSION NO. 3

FINAL TEMP. CALCULATED = 320.33
FINAL TEMP. MEASURED = 319.24

COMPUTED VALUE OF GAMMA = 1.5998

TIME	PRESSURE	TEMPERATURE	CONSTANT	PERCENT DEV.
0.00	529.8	293.66	27.960	0.000
.10	667.0	319.50	27.904	-.200
.15	662.5	319.33	27.960	-.000
.20	662.0	319.50	27.983	.082
.25	662.1	319.33	27.965	.018
.30	660.9	319.15	27.970	.036
.35	660.2	318.98	27.965	.019
.40	663.4	319.24	27.938	-.079
.45	661.9	319.06	27.947	-.048
.50	662.3	318.89	27.925	-.125
.55	662.1	318.63	27.904	-.201
.60	662.3	318.45	27.887	-.262
.65	662.1	318.28	27.873	-.310
.70	662.1	318.02	27.851	-.389
.75	662.1	317.67	27.821	-.498
.80	662.1	317.41	27.797	-.584

COMPRESSION NO. 4

FINAL TEMP. CALCULATED = 321.32
FINAL TEMP. MEASURED = 320.29

COMPUTED VALUE OF GAMMA = 1.6031

TIME	PRESSURE	TEMPERATURE	CONSTANT	PERCENT DEV.
0.00	529.6	293.66	27.738	0.000
.10	667.0	320.29	27.738	.000
.15	666.0	320.29	27.753	.057
.20	666.4	320.46	27.762	.086
.25	666.2	320.37	27.758	.074
.30	665.0	320.20	27.761	.083
.35	665.6	320.20	27.752	.051
.40	665.9	320.11	27.740	.008
.45	666.8	320.11	27.725	-.045
.50	666.2	319.85	27.713	-.089
.55	666.3	319.59	27.688	-.180
.60	666.2	319.33	27.667	-.256
.65	666.1	319.15	27.653	-.304
.70	665.9	318.80	27.627	-.401
.75	665.9	318.63	27.611	-.455
.80	665.9	318.19	27.574	-.592

COMPRESSION NO. 5

FINAL TEMP. CALCULATED = 320.74
FINAL TEMP. MEASURED = 320.02

COMPUTED VALUE OF GAMMA = 1.6138

TIME	PRESSURE	TEMPERATURE	CONSTANT	PERCENT DEV.
0.00	529.3	293.66	27.033	0.000
.10	664.6	320.02	27.015	-.064
.15	663.4	320.02	27.033	.003
.20	663.5	320.02	27.033	.000
.25	663.4	320.11	27.041	.030
.30	662.6	319.94	27.038	.021
.35	666.4	320.46	27.024	-.032
.40	663.9	320.20	27.040	.029
.45	663.6	319.94	27.023	-.037
.50	664.0	319.68	26.995	-.138
.55	664.1	319.50	26.979	-.199
.60	664.2	319.15	26.948	-.311
.65	664.0	319.06	26.944	-.329
.70	663.9	318.72	26.915	-.435
.75	663.9	318.45	26.893	-.516
.80	663.9	318.19	26.871	-.598

COMPRESSION NO. 6

FINAL TEMP. CALCULATED = 318.77
FINAL TEMP. MEASURED = 317.49

COMPUTED VALUE OF GAMMA = 1.5904

TIME	PRESSURE	TEMPERATURE	CONSTANT	PERCENT DEV.
0.00	529.0	293.66	28.632	0.000
.10	656.5	316.97	28.526	-.373
.15	652.2	317.32	28.626	-.023
.20	652.2	317.41	28.635	.007
.25	652.8	317.49	28.632	.000
.30	652.2	317.41	28.634	.004
.35	651.2	317.23	28.634	.006
.40	652.2	317.41	28.634	.004
.45	653.9	317.49	28.614	-.063
.50	653.1	317.32	28.611	-.074
.55	653.4	317.14	28.592	-.142
.60	653.4	316.97	28.576	-.197
.65	653.4	316.79	28.560	-.251
.70	653.4	316.62	28.545	-.306
.75	653.4	316.45	28.529	-.361
.80	653.4	316.18	28.505	-.444

COMPRESSION NO. 7

FINAL TEMP. CALCULATED = 315.14
FINAL TEMP. MEASURED = 314.96

COMPUTED VALUE OF GAMMA = 1.6314

TIME	PRESSURE	TEMPERATURE	CONSTANT	PERCENT DEV.
0.00	528.5	293.66	25.940	0.000
.10	636.7	313.91	25.800	-.539
.15	632.9	314.79	25.931	-.032
.20	633.3	314.96	25.940	.000
.25	634.7	315.22	25.939	-.002
.30	633.8	315.05	25.939	-.003
.35	633.1	314.87	25.936	-.014
.40	634.4	315.22	25.944	.019
.45	635.6	315.22	25.926	-.053
.50	635.8	315.14	25.915	-.094
.55	636.0	315.05	25.905	-.135
.60	636.1	314.87	25.889	-.197
.65	636.2	314.79	25.880	-.228
.70	636.3	314.70	25.872	-.263
.75	636.4	314.61	25.862	-.300
.80	636.6	314.35	25.838	-.394

```
 12 FORMAT(6F10.2)
 14 FORMAT(I2)
 15 FORMAT(4I2)
 17 FORMAT(3X,F7.2,F13.1,F17.2,F12.1,///)
 22 FORMAT(3I3)
800 FORMAT(6X,24HFINAL TEMP. CALCULATED =,F7.2)
801 FORMAT(6X,22HFINAL TEMP. MEASURED =,F7.2//)
802 FORMAT(6X,25HCOMPUTED VALUE OF GAMMA =,F9.4///)
803 FORMAT(1H+,5X,4HTIME,5X,8HPRESSURE,5X,11HTEMPERATURE)
804 FORMAT(3X,F7.2,F11.1,F15.2,F15.3,F16.3//)
805 FORMAT(44X,8HCONSTANT,5X,12HPERCENT DEV.//)
900 FORMAT(4X,4HDATE,1X,I2,1H/,I2,1H/,I2,3X,14HEXPERIMENT NO.,I2///)
904 FORMAT(1H+,4X,24HINCHES  INITIAL PRESSURE,6X,13HINCHES  FINAL)
905 FORMAT(49X,8HPRESSURE)
908 FORMAT(1H1)
910 FORMAT(1H7)
920 FORMAT(21X,16HCALIBRATION DATA)
925 FORMAT(10X(15HCOMPRESSION NO.,I2///)
930 FORMAT(1H )
    PRINT 908
    PRINT 910
    PRINT 930
    READ 15,LD,LM,LY,LEXP
    PRINT 900,LD,LM,LY,LEXP
    READ 12,BP
    READ 12,T1
    PRINT 920
    PRINT 904
    PRINT 905
    GAM=1.64
    A=(1.-GAM)/GAM
    READ 12,XI,YI,XF,YF
    READ 12,SLOPE,XTI
    PRINT 17,XI,YI,XF,YF
    EMI=5.347
    EMF=5.564
```

```
      BI=YI-EMI*XI+BP
      BF=YF-EMF*XF+BP
      READ 14,NUB1
      READ 14,NUB2
      NO=0
      DO 60 N=1,NUB1
      READ 22,NRAPI,NRAPF,NXT
      XT=NXT
      RAPI=NRAPI
      RAPF=NRAPF
      NO=NO+1
      API=(EMI*RAPI/100.+BI)
      APF=(EMF*RAPF/100.+BF)
      RPRES=API/APF
      PRINT 925,NO
      T2C=T1*((RPRES)**A)
      PRINT 800,T2C
      T2M=T1+SLOPE*(XT/100.-XTI)
      PRINT 801,T2M
      RTEMP=T2M/T1
      GAMC=1./((LOGF(RTEMP)/LOGF(RPRES))+1.)
      A2=(1.-GAMC)/GAMC
      PRINT 802,GAMC
      PRINT 908
      PRINT 910
      PRINT 930
      XONST= T1*(API**A2)
      PRINT 803
      PRINT 805
      TIME=0.
      DEV=0.
      PRINT 804,TIME,API,T1,XONST,DEV
      TIME=0.05
      DO 50 M=1,NUB2
      READ 22,NRAPF,NXT
      XT=NXT
```

```
      RAPF=NRAPF
      APF=(EMF*RAPF/100.+BF)
      T2M=T1+SLOPE*(XT/100.-XTI)
      CONST=T2M*(APF**A2)
      DEV=((CONST-XONST)*100.)/XONST
      TIME=TIME+0.05
   50 PRINT 804,TIME,APF,T2M,CONST,DEV
      PRINT 908
      PRINT 910
      PRINT 930
   60 CONTINUE
      STOP
      END
```

APPENDIX II

LIST OF SYMBOLS

T_1 = Initial Temperature in Cloud Chamber

T_2 = Final Temperature in Cloud Chamber After Adiabatic Change of State

P_1 = Initial Pressure in Cloud Chamber

P_2 = Final Pressure in Cloud Chamber After Adiabatic Change of State

V_1 = Initial Volume in Cloud Chamber

V_2 = Final Volume in Cloud Chamber After Adiabatic Change of State

ρ_o = Saturation Vapor Density at T_1

ρ_∞ = Saturation Vapor Density at T_2

ρ_2 = Vapor Density After Adiabatic Change of State

p_o = Saturation Vapor Pressure at T_1

p_∞ = Saturation Vapor Pressure at T_2

p_2 = Vapor Pressure After Adiabatic Change of State

γ = Ratio of Heat Capacities c_p/c_v

μ_1 = Chemical Potential of Water in the Liquid Phase

μ_v = Chemical Potential of Water in the Vapor Phase

G = Gibbs Free Energy

S = Entropy

$\overline{S}$ = Molar Entropy

$\overline{V}$ = Molar Volume

Δ = Most Probable Error

δ = Standard Deviation

p_g = Vapor Pressure of Helium

p_v = Vapor Pressure of Water Vapor

P = Total Pressure of p_g and p_v

S = Supersaturation (not to be confused with entropy used above)

BIBLIOGRAPHY

BIBLIOGRAPHY

1. C. W. Mettenburg, "An Improved Long Sensitive Time Wilson Cloud Chamber," M.S. Thesis, University of Missouri at Rolla, (1958).
2. D. A. Rinker, "A Study of Background in a Long Sensitive Time Wilson Cloud Chamber," M.S. Thesis, University of Missouri at Rolla, (1958).
3. J. B. Hughes, "A Preliminary Search for Subionizers," M.S. Thesis, University of Missouri at Rolla, (1959).
4. E. F. Allard, "A New Determination of the Homogeneous Nucleation Rate of Water in Helium," Ph.D. Dissertation, University of Missouri at Rolla, (1964).
5. Van Heerden, "The Threshold Expansion Ratio of Water Vapour," Physica, XIII, no. 1-3, pp.41-46, (1947).
6. W. G. Courtney, Kinetics of Condensations of Water Vapor, Quarterly Report, Texaco Experiment, Inc., (1964).
7. J. L. Kassner, Experimental and Theoretical Studies of Nucleation Phenomena, Research Proposal Submitted to the National Science Foundation (1964).
8. J. C. Carstens and R. Buecher, private communication.
9. International Critical Tables of Numerical Data, Physics, Chemistry, and Technology (McGraw-Hill Book Company Inc,, New York, 1926).
10. N. N. Das Gupta and S. K. Ghosh, "A Report on the Wilson Cloud Chamber and Its Applications in Physics,"

Rev. Mod. Phys. 18, 2 (1946).

11. R. J. Schmitt, "A Second Study of the Homogeneous Nucleation Rate of Water Vapor in Helium," M.S. Thesis, University of Missouri at Rolla, (1965).

12. R. Dawbarn, "A Study of Re-evaporation Nuclei," M.S. Thesis, University of Missouri at Rolla, (1965).

13. M. A. Grayson, "A Measurement of Dead Space and Its Effect On Homogeneous Nucleation Rate of Water Vapor in Helium," M.S. Thesis, University of Missouri at Rolla, (1965).

14. G. W. Castellan, Physical Chemistry. Addison-Wesley, Reading, Mass., p.243, (1964).

15. F. Richarz, "The Value of the Ratio of Specific Heats For a Mixture of Two Gases," Ann. d. Physik 19,639 (1906).

16. M. P. Vulkalovitch, Thermodynamic Properties of Water and Steam, State Publishing House of Scientific-Technical Literature Concerning Mechanical Engineering, Moscow, (1958).

17. O. D. B. Mann, The Thermodynamic Properties of Helium From 3 to 300°K Between 0.5 and 100 Atmospheres, National Bureau of Standards Technical Note 154, U. S. Government Printing Office, (1962).

18. L. Katz, S.B. Woods, and A.L. Clark, "The Resonance Method of Measuring the Ratio of the Specific Heats of a Gas, Can. J. Research, A, 18:22, (1940).

19. R. Dawbarn, private communication.

VITA

The author was born August 6, 1940 to Ella T. and Eugene S. Packwood in Golden City, Missouri. He received his elementary education in the public schools of Golden City and St. Joseph, Missouri. He attended Central High School of St. Joseph and received his diploma June, 1958.

In September, 1958, he entered the University of Missouri School of Mines and Metallurgy, Rolla, Missouri. He received his B. S. degree in Physics from the University of Missouri School of Mines and Metallurgy in June, 1963.

He entered the Graduate School of the University of Missouri at Rolla in June, 1963 as a candidate for the degree of Master of Science in Physics.